UNIVERSIDADE D
COIMBRA

Joaquim António Maximiano Gomes

Perturbações de curvatura geradas durante a inflação térmica

Dissertação no âmbito do Mestrado em Física, ramo de Física Nuclear e de Partículas orientada pelo Professor Doutor João Pedro Trancoso Gomes Rosa e apresentada ao Departamento de Física da Faculdade de Ciências e Tecnologia.

Outubro de 2020

UNIVERSIDADE D
COIMBRA

October 2020

Curvature perturbations from thermal inflation

Joaquim António Maximiano Gomes

UNIVERSIDADE D
COIMBRA

supervised by Prof. Dr. João Pedro Trancoso Gomes Rosa

Department of Physics
University of Coimbra
Portugal

Dedicada
à Adelaide, ao Joaquim e à Helena
e também à Joana

pelo amor que me dão

Agradecimentos

Queria agradecer principalmente ao professor João Rosa, o meu orientador, pelas tardes a discutir física que foram indispensáveis para levar esta tese a bom porto, bem como às suas correções e sugestões que foram imprescindíveis.

Agradeço também à Joana pela sua paciência e apoio durante todo este ano, e por me ter dado sugestões valiosas.

Um obrigado especial ao Guilherme pela sua vontade em rever a minha tese.

Um profundo obrigado à minha família, Adelaide, Joaquim, Maria Helena e Helena Maria por terem sempre estado aqui para mim.

Agradeço ao Francisco, que é como meu irmão, e ao Tiago pela sua amabilidade.

Também quero agradecer fortemente à minha outra família, Elsa, Mário, Leonor, João, Carolina e Miguel.

Um obrigado ao meu amigo Raphael por tudo aquilo que ele me ensinou.

Relembro o Guilherme e o Pedro, os meus amigos de licenciatura, e o António, o grande amigo que conheci em Coimbra.

No final, mas com igual relevo, agradeço ao Luís, à Maria, ao Alexandre, ao Diogo, à Susana, ao Ivo, ao Ricardo, ao Miguel e ao João que me acompanharam neste último ano.

Abstract

An early epoch of inflation in the cosmic history is now taken as paradigmatic since it eliminates the apparent fine-tuning of the standard cosmological model. Moreover, it can explain the small inhomogeneities of the cosmic microwave background. In addition to the main period of inflation, certain supersymmetric theories predict a class of scalar fields with an extremely flat potential, known as flatons. These fields can drive a shorter secondary inflationary period when they are held in a metastable vacuum state by thermal effects. Such a period of thermal inflation may dilute away any dangerous relics, such as gravitinos and moduli, that can be copiously produced during reheating, at the end of the first inflationary epoch.

As thermal inflation occurs after the main inflation ends, it can produce perturbations in the curvature of space-time at smaller cosmological scales. Such perturbations could, in principle, have considerably larger amplitude than the large-scale perturbations observed in the cosmic microwave background. In fact, large enough perturbations could collapse directly into primordial black holes upon horizon re-entry in the radiation era. These astronomical objects are leading candidates for (at least a fraction of) the dark matter in the universe.

In this thesis we have investigated the spectrum of space-time curvature perturbations during thermal inflation, generated by fluctuations of the flaton field. A recent study in the literature considered only quantum fluctuations of the said field, while thermal considerations were practically disregarded. However, even though the flaton is the dominant fluid during this period, it coexists and interacts with a subdominant radiation bath. As a result the flaton should exhibit fluctuation-dissipation dynamics that cannot be ignored. This will make the flaton evolve towards a state of thermal equilibrium, provided that the interaction rate exceeds the Hubble expansion rate. This effectively results in the flaton field behaving like a stochastic classical field instead of as a quantum field.

With this in mind, we have studied the evolution of thermal perturbations produced by the flaton in the curvature of space-time, as it approaches equilibrium with a thermal bath. We have computed the power spectrum of the curvature perturbations and found that it is smaller than the purely quantum one previously studied in the literature. In fact, we have found that the presence of the radiation bath severely

suppresses the amplitude of the curvature perturbations that may be created during thermal inflation. This makes it, therefore, very hard to form an appreciable primordial black hole population by curvature perturbations generated during this period.

Keywords: cosmology; thermal inflation; fluctuation-dissipation theorem; curvature perturbations; primordial black holes

Resumo

Um período de inflação no início da história cósmica é agora tomado como paradigmático, visto este eliminar a aparente forte dependência da cosmologia padrão nas suas condições iniciais. Além disso, consegue explicar as pequenas heterogeneidades da radiação cósmica de fundo. Para além da época principal de inflação, algumas teorias supersimétricas preveem uma classe de campos escalares com um potencial extremamente plano, conhecidos como flatões. Estes campos podem levar a cabo um período secundário de inflação, mais curto que o primeiro, onde os referidos campos são mantidos num vácuo metastável por efeitos térmicos. Este período de inflação térmica pode diluir artefactos cosmológicos, como gravitinos e *moduli*, que podem ser produzidos em abundância durante o reaquecimento que segue a inflação principal.

Visto que a inflação térmica ocorre depois da inflação primária ter terminado, esta pode levar à produção de perturbações na curvatura do espaço-tempo a escalas cosmológicas mais pequenas. Estas perturbações podem, em princípio, ter uma magnitude consideravelmente maior que as perturbações a larga escala observadas na radiação cósmica de fundo. Com efeito, perturbações suficientemente grandes podem colapsar diretamente em buracos negros quando reentram através do horizonte, na era de radiação. Estes buracos negros primordiais são, portanto, candidatos proeminentes a constituir (pelo menos uma parte) a matéria escura no universo.

Na presente tese investigámos qual o espectro das perturbações da curvatura do espaço-tempo induzido pelas flutuações do flatão durante a inflação térmica. Um estudo recente considerou apenas flutuações quânticas do campo referido, desconsiderando praticamente os efeitos da temperatura. No entanto, mesmo que o flatão seja o fluido mais abundante durante este período, ele coexiste e interage com um banho térmico subdominante. Isto significa que o flatão deve exibir uma dinâmica de flutuação-dissipação que não pode ser descartada. Estas farão o flatão evoluir para um estado de equilíbrio térmico, desde que a taxa de interação seja superior à taxa de expansão de Hubble. Efetivamente, isto faz com que o flatão se comporte como um campo clássico estocástico em vez de como um campo quântico.

Com isto em mente, estudámos a evolução das perturbações térmicas criadas pelo flatão na curvatura do espaço-tempo, à medida que este tende para o equilíbrio com o banho térmico. Calculámos o espectro das perturbações e descobrimos que estas são

mais pequenas que o exposto no estudo puramente quântico estudado anteriormente na literatura. De facto, constatámos que a presença de um banho térmico suprime severamente a amplitude das perturbações da curvatura geradas durante a inflação térmica. Neste sentido, será difícil que uma população considerável de buracos negros primordiais tenha sido criada por perturbações na curvatura geradas durante esse período.

Palavras-chave: cosmologia; inflação térmica; teorema de flutuação-dissipação; perturbações de curvatura; buracos negros primordiais

ἁρμονίη ἀφανὴς φανερῆς κρείττων

harmonia inaparente
mais forte que a aparente

Ἡράκλειτος ὁ Ἐφέσιος (Heraclito de Éfeso)

Contents

List of Figures

List of Tables

Chapter 1

Introduction

The standard cosmological model is extremely successful in describing how the universe evolved from an initially hot and dense state into its present configuration, after nearly 14 billion years of expansion. It presupposes a largely homogeneous and isotropic universe that expanded according to Einstein's theory of general relativity, with an energy balance dominated first by radiation, then by non-relativistic matter (including both dark and baryonic matter) and presently by a mysterious cosmological constant that is accelerating expansion. This simple model accurately predicts the cosmic abundances of light nuclear elements and the black body spectrum of the cosmic microwave background (CMB) at 2.73K.

The CMB's remarkable isotropy and homogeneity, however, constitute an intriguing puzzle, since at least according to standard cosmology, most regions in the presently observable universe have never been in causal contact before. So how they all happen to be at the same temperature today, with only small fluctuations of a few microkelvin? Is such a fine-tuning in the initial conditions acceptable in a physical theory? Moreover, the typical angular scale of CMB fluctuations in the night sky also tells us that the present universe has a very small spatial curvature, which again points towards a severe fine-tuning of its initial state.

It is now widely believed that an early epoch of inflation would solve this initial conditions problem, as well as explaining the small inhomogeneities that we observe in the cosmic microwave background, which will later seed the large-scale structure in the universe [1, 2, 3, 4]. Inflation corresponds to a period of accelerated expansion where an initially small homogeneous region expands by a huge factor and becomes much larger than the causal horizon. Resulting in any initial spatial curvature vanishing, therefore solving the above-mentioned problems. Inflation also dilutes away any dangerous relics such as monopoles (a type of topological defect) that are predicted in fundamental high-energy theories such as grand unified theories [2].

However, inflation is necessarily followed by a reheating process that brings the universe into the initial hot and dense state of standard cosmology. This process is

thought to involve the decay of the inflaton scalar field responsible for inflation into ordinary standard model particles and possibly dark matter or other exotic species. In fact, in supersymmetry/supergravity theories, which are thought to constitute the low-energy limit of string/M-theory, the reheating process typically generates other dangerous relics such as gravitinos, gauge monopoles or moduli fields that could spoil the successful predictions of standard cosmology.

An epoch of thermal inflation has been proposed to address these issues [5, 6], taking advantage of the plethora of scalar fields predicted in supergravity/string theory. One of these so-called flaton fields may be temporarily stuck in a metastable minimum by thermal effects and act as a cosmological constant during a short period, thus inflating away any dangerous relics produced after the first inflationary epoch.

As it occurs after the main inflation period, thermal inflation will generate space-time curvature perturbations at scales much shorter than those observed in the cosmic microwave background. These perturbations would be brought about by fluctuations in the flaton field itself, and could be much larger than the CMB's inhomogeneities. In fact, if large enough, they could collapse directly into primordial black holes [7], which could account for at least a fraction of dark matter or even possibly the gravitational waves recently detected by LIGO/Virgo [8, 9].

This was previously considered in [10] but its analysis regarded the flaton as a quantum field at zero temperature. As in this epoch temperature is clearly relevant we should treat the flaton as a quantum field at a finite temperature, which curiously will turn it into a stochastic classical field. If we are to expect perturbations from the flaton we must postulate that it starts out of equilibrium and then evolves towards it due to its interaction with the ambient radiation bath. To accomplish this we will use the formalism of thermal field theory [11, 12] and fluctuation-dissipation dynamics [13, 14] to study the evolution of the flaton's fluctuations throughout thermal inflation and obtain the power spectrum of space-time curvature perturbations on super-horizon scales. We can then compare our results with its quantum analog computed in [10] and observe if how the thermal fluctuations compare with the purely quantum ones.

In the remainder of this chapter we present our physical units and mathematical conventions. In chapter 2 we discuss the basics of standard cosmology and in chapter 3 we explain what inflation has meant to our understanding of the universe. We devote chapter 4 to the dynamics of a period of thermal inflation driven by a flaton field. We describe how the flaton evolves towards equilibrium with the ambient radiation bath in chapter 5. All this is set up to ultimately compute the power spectrum of curvature perturbations induced by the flaton in chapter 6. Finally, in chapter 7, we summarize and discuss our results, commenting on possible improvements and future directions of research.

1.1 Conventions

We will use natural units with $c = \hbar = k_B = \frac{1}{4\pi\epsilon_0} = 1$. Allowing any base unit to be given in units of energy. We will use GeV for the units of energy but the reduced Planck mass $M_p = \frac{1}{\sqrt{8\pi G}} = 2.435 \times 10^{18}$ GeV will also be relevant. Below in table 1.1 we present the base physical quantities in natural units.

Table 1.1: Base physical quantities in natural units.

base quantity	**natural unit**
energy	GeV^1
length	GeV^{-1}
time	GeV^{-1}
temperature	GeV^1
charge	1

We will use the signature $(-,+,+,+)$ for the space-time metric. Repeated indices are summed over. Latin letter indices run over the three spatial coordinates labeled $1, 2, 3$ and the greek letter indices run over the four space-time coordinates, where the zeroth component is time.

Three-vectors are denoted in boldface and four-vectors are written in plain text. For example the position vector in three dimensional space is $\boldsymbol{x}$, while the position four-vector is x.

We also follow the dot notation for the time derivative, $\dot{f} = \frac{df}{dt}$.

Finally we define the Fourier transform of a function of space $f(\boldsymbol{x})$ as in [3]:

$$f_k(\boldsymbol{k}) = \int_{-\infty}^{\infty} d^3x\, f(\boldsymbol{x}) \exp(-i\boldsymbol{k}\cdot\boldsymbol{x}) \tag{1.1}$$

and the inverse Fourier transform has to be:

$$f(\boldsymbol{x}) = \int_{-\infty}^{\infty} \frac{d^3k}{(2\pi)^3}\, f_k(\boldsymbol{k}) \exp(i\boldsymbol{k}\cdot\boldsymbol{x}). \tag{1.2}$$

Below in table 1.2 we present composite physical quantities common in this work in natural units, so that one can easily verify the dimensional consistency of the expressions.

Table 1.2: Physical composite quantities in natural units.

composite quantity	**natural unit**
H (Hubble parameter)	GeV^{1}
ϕ (real scalar field)	GeV^{1}
ϕ_k (Fourier modes of a real scalar field)	GeV^{-2}
ξ (noise field)	GeV^{3}
ξ_k (Fourier modes of the noise field)	1

Chapter 2

Standard cosmology

Cosmology studies the evolution of the universe as a whole, inquiring about its beginning and trying to predict its end. There are many good sources for the understanding of this subject [1, 15, 16, 17], notwithstanding, in this chapter we will give a brief overview of cosmology.

If we were looking at the night sky a couple of millennia ago with no technology but our eyes to inquire the dispositions of the heavenly bodies, we could say that even though the fixed stars seemed to wander periodically around the night in the timespan of a year, that the universe was unchanging and eternal. This was the enduring cosmological view until two facts changed it from a philosophical matter, inaccessible to experiment, to a rigorous science that could make accurate predictions about the universe. In 1929, Edwin Hubble published a paper where he showed that there was a linear relation between the radial distance of extra-galactic nebulae and their radial velocity [18]. This was soon interpreted as the fact that the universe is expanding – its length scale is growing as time goes on. The other formidable discovery was the measurement of a constant microwave radiation emanating isotropically from all the night sky, now known as the cosmic microwave background or CMB for short [19]. The CMB's spectrum is Planckian with a precision of one part in 10^5 [4], which enables us to associate with it a temperature. This is what is meant when one says that the present temperature of the universe is roughly $3\,\mathrm{K}$ [20, 21]. This reveals us that besides the usual matter comprising known astronomical bodies like galaxies and stars there also exists an energy density that fills the universe in the form of radiation.

From these two important empirical facts we can construct a model describing not only how our universe is but also how it has evolved into what we presently observe. This is called the standard cosmology.

2.1 An expanding universe

Our universe seems to be homogeneous and isotropic at large scales. Homogeneous in the sense that every point in the universe is indistinguishable from any other, isotropic because an observer in any point would see the same universe regardless of the direction she looked at. These beliefs are founded on induction and in the fact that models supported by these claims seem to describe well the real world. As a matter of fact it is hard to prove homogeneity and isotropy at large scales because we as humans have only a very limited portion of the universe available to us. Nevertheless modern observations like the isotropy of the CMB appear to align well with a homogeneous and isotropic universe at large scales [22, 23].

The universe can be described by a four-dimensional Lorentzian manifold with a metric $g_{\mu\nu}$. However, because it is expanding the claims of isotropy and homogeneity will only hold on a spatial tridimensional submanifold defined at each instant of time, described by the metric γ_{ij}. These assumptions translate into the fact that the spatial manifold must be maximally symmetric because such a universe will have rotational and translational symmetries, hence the maximum number of Killing vectors [22]. This allow us to posit the following metric:

$$ds^2 = g_{\mu\nu}dx^\mu dx^\nu = -dt^2 + R^2(t)\gamma_{ij}(u)du^i du^j, \tag{2.1}$$

where t is the time-like coordinate, $R(t)$ is a scale factor that indicates how the length scale of the universe evolves with time. The components $\{u^i\}$ are named comoving coordinates, being those that make the metric free of any $dtdu^i$ cross terms and make the coefficient of dt^2 independent of u^i.

The Riemann tensor associated with the maximally symmetric 3-dimensional metric γ_{ij} is given by [22]:

$$^{(3)}R_{ijkl} = k(\gamma_{ik}\gamma_{jl} - \gamma_{il}\gamma_{jk}), \tag{2.2}$$

where we have defined:

$$k = \frac{^{(3)}R}{6}. \tag{2.3}$$

The quantity $^{(3)}R$ is the Ricci scalar (A.7). The superscript $^{(3)}$ reminds us that this geometry concerns the tridimensional submanifold mentioned above.

The Ricci tensor (A.6) associated with (2.2) is:

$$^{(3)}R_{ij} = 2k\gamma_{ij}. \tag{2.4}$$

If the spatial manifold is maximally symmetric then it should be spherically symmetric with a metric of the form:

$$\gamma_{ij}(u)du^i du^j = \exp[2\beta(\rho)]d\rho^2 + \rho^2 d\Omega^2, \tag{2.5}$$

where $d\Omega^2 = d\theta^2 + \sin^2\theta d\phi^2$ is the metric of a two-sphere. We are only free to parameterize the radial part because changing the coefficient of $d\Omega^2$ would spoil the spherical symmetry. We use an exponential so that the metric signature remains $(-,+,+,+)$.

We can now compute the Christoffel symbols associated with the above metric (2.5) then use them to compute the Riemann and Ricci tensors, as done in [22]. The non-zero components of the Ricci tensor are:

$$\begin{aligned} {}^{(3)}R_{11} &= \frac{2}{\rho}\partial_1\beta, \\ {}^{(3)}R_{22} &= 1 + \exp(-2\beta)(\rho\partial_1\beta - 1), \\ {}^{(3)}R_{33} &= \sin^2\theta\left[1 + \exp(-2\beta)(\rho\partial_1\beta - 1)\right]. \end{aligned} \tag{2.6}$$

Comparing with (2.4) we constrain $\beta(\rho)$ to satisfy:

$$\exp(2\beta) = \frac{1}{1 - k\rho^2}, \tag{2.7}$$

yielding the metric:

$$ds^2 = -dt^2 + R^2(t)\left(\frac{d\rho^2}{1 - k\rho^2} + \rho^2 d\Omega^2\right), \tag{2.8}$$

named Friedmann–Lemaître–Robertson–Walker metric or Robertson–Walker metric for short.

As the type of geometry is just defined by whether k is positive, negative or zero, we commonly let the magnitude of k be absorbed into ρ and just consider $k \in (-1, 0, 1)$.

The case $k = 0$ gives a space with no curvature at all so the spatial tridimensional manifold will be $\mathbb{R}^3$, called flat. For $k = 1$ the manifold has positive curvature and is called closed. Lastly when $k = -1$ the manifold has negative curvature and it is called open.

This metric is invariant with respect to the transformation:

$$\begin{aligned} R &\to \lambda^{-1}R, \\ \rho &\to \lambda\rho, \\ k &\to \lambda^{-2}k, \end{aligned} \tag{2.9}$$

where λ is a constant real parameter. We will follow the standard approach of restoring length units to the radial coordinate and make the scale factor adimensional:

$$\begin{aligned} R &\to \frac{R}{R_0} \equiv a(t), \\ \rho &\to R_0\rho \equiv r, \\ k &\to R_0^{-2}k \equiv \kappa, \end{aligned} \tag{2.10}$$

where $a(t)$ is the adimensional scale factor. This forcefully gives units of (length)$^{-2}$ to κ and allows it to take any value. In spite of this, the sign of κ is still what describes the geometry of the spatial hypersurfaces.

This change yields:

$$ds^2 = -dt^2 + a^2(t)\left(\frac{dr^2}{1-\kappa r^2} + r^2 d\Omega^2\right). \tag{2.11}$$

We pause here to note that there are various sources of evidence that our universe is flat to a great degree of precision, with the Planck satellite in particular yielding an upper bound of $\kappa \leq 10^{-11}\,\text{Mpc}^{-2}$ [24].

To understand the consequences of an expanding universe, suppose that a galaxy that is not bound to our own is a radial distance r from us. Since the universe expanding we can consider some reference length R_0 and say:

$$r(t) = R_0 a(t), \tag{2.12}$$

this means that its radial velocity v is

$$v = r\frac{\dot{a}}{a} \equiv H(t)r, \tag{2.13}$$

where $H(t)$ is the Hubble parameter and (2.13) is Hubble's law as originally stated by Edwin Hubble himself in his 1929 paper[1].

The current value of the Hubble parameter is denoted by H_0 and usually called Hubble constant. It is commonly written in terms of the dimensionless Hubble parameter h, such that:

$$H_0 = 100h\ \text{km}\,\text{s}^{-1}\text{Mpc}^{-1} \tag{2.14}$$

and a current value is $h = 0.6766 \pm 0.0042$ [24].

The Hubble parameter has units of time^{-1} and so reverting momentarily to the international system of units (SI) we can obtain a length and a time from H_0. The Hubble length d_H:

$$d_H = H^{-1}c, \tag{2.15}$$

gives a typical length in the universe and the Hubble time:

$$t_H = H^{-1}, \tag{2.16}$$

gives the temporal scale of the universe. These quantities vary with time, which means that the typical cosmological scales might be very different in the past, present or future. The Hubble length is also referred to as the Hubble horizon because it gives us the present causality horizon. Regions a distance d_H from us are receding at the speed of light so are outside our present light cone.

[1] It is important to note that (2.13) only holds in this linear form for short distances, that is, a more complete relation will have non-linear terms [1]. Also note that this simple exposition is only strictly true for a comoving observer.

2.2 Matter and energy in the universe

The existence of a cosmic microwave background tells us that radiation makes up part of our universe. Our observations of galaxies composed of stars, planets, other astronomical objects and ourselves for that matter are examples of ordinary non-relativistic matter. We now complete the picture given above – the universe is described by a four dimensional manifold with a Robertson-Walker metric (2.11) and it is related to the matter and energy content of the universe through Einstein's equation [16, 22, 23]:

$$G_{\mu\nu} = M_p^{-2} T_{\mu\nu}, \tag{2.17}$$

where $G_{\mu\nu}$ is the Einstein tensor (A.8) which is a function of the metric, and $T_{\mu\nu}$ is the energy-momentum tensor which describes the local matter and energy content of the region under consideration, in the case of cosmology, the entire universe. It is given by[4, 22]:

$$T_{\mu\nu} = -\frac{2}{\sqrt{-g}} \frac{\delta S_M}{\delta g^{\mu\nu}}, \tag{2.18}$$

where g is the determinant associated with the matrix representation of $g_{\mu\nu}$ and S_M stands for the action of any intervening matter fields.

Einstein's equation (2.17) is in fact a set of coupled, non-linear differential equations, and so the metric and the content of the universe are mutually dependent. Nevertheless we will consider the metric of the universe as a fixed Robertson-Walker metric (2.11) that follows from the general assumptions of homogeneity and isotropy, which we take to hold for all times.

To obtain the simplest model of the universe, it is common practice to treat the energy content in the universe as a perfect fluid which has the associated energy-momentum tensor [22]:

$$T^{\mu\nu} = (\rho + p) U^\mu U^\nu + p g^{\mu\nu}, \tag{2.19}$$

where ρ is the energy density and p is the pressure of the fluid, while U^μ is its four-velocity. The trace of a $(0, 2)$ tensor A is given by $A^\mu{}_\mu = A^{\mu\nu} g_{\mu\nu}$. For the case of (2.19) this gives:

$$T^\mu{}_\mu = -\rho + 3p. \tag{2.20}$$

If the Robertson-Walker metric is isotropic in comoving coordinates then the fluid should also be isotropic in the same coordinates. This means that the fluid is at rest in comoving coordinates, having the following four-velocity:

$$U^\mu = (1, 0, 0, 0). \tag{2.21}$$

With this in mind we can now find a set of differential equations relating the dimensionless scale factor $a(t)$ from the Robertson-Walker metric (2.11) and the energy

density and pressure of the perfect fluid. Thus liking the expansion of the universe with its matter and energy content.

This is obtained by means of Einstein's equation. The components of the Einstein tensor for the Robertson-Walker metric (B.5) being:

$$\begin{aligned} G_{00} &= 3\left(\frac{\dot{a}^2}{a^2} + \frac{\kappa}{a^2}\right), \\ G_{ij} &= -\left(\frac{2\ddot{a}}{a} + \frac{\dot{a}^2}{a^2} + \frac{\kappa}{a^2}\right) g_{ij}. \end{aligned} \tag{2.22}$$

Equating this to (2.19) using Einstein's equation (2.17), we obtain:

$$\begin{aligned} H^2 &= \frac{\rho}{3M_p^2} - \frac{\kappa}{a^2}, \\ \frac{2\ddot{a}}{a} &= -\frac{p}{M_p^2} - H^2 - \frac{\kappa}{a^2}. \end{aligned} \tag{2.23}$$

Finally, we use the first equation to rewrite the second one and we obtain the pair of equations:

$$H^2 = \frac{\rho}{3M_p^2} - \frac{\kappa}{a^2}, \tag{2.24a}$$

$$\frac{\ddot{a}}{a} = -\frac{1}{6M_p^2}(\rho + 3p). \tag{2.24b}$$

Where the first is known as Friedmann equation and the second as Raychaudhuri or acceleration equation. A universe where fluids satisfy the Friedmann equation is called Friedmann–Lemaître–Robertson–Walker universe or Robertson–Walker universe for short and is the simplest description of a universe that is everywhere homogeneous and isotropic.

An important quantity is the density parameter or abundance:

$$\Omega \equiv \frac{1}{3H^2M_p^2}\rho = \frac{\rho}{\rho_{\text{crit}}}, \tag{2.25}$$

where ρ_{crit} is the critical density defined as the density the universe must have in order to be flat:

$$\rho_{\text{crit}} = 3H^2M_p^2. \tag{2.26}$$

As we can see when one rewrites Friedmann equation (2.24a) using the density parameter:

$$\Omega - 1 = \frac{\kappa}{a^2H^2}. \tag{2.27}$$

We note that sometimes the curvature term is considered as a spurious energy density (2.27):

$$\Omega + \Omega_\kappa = 1, \tag{2.28}$$

where Ω_κ is the density parameter associated with curvature defined as:

$$\Omega_\kappa = -\frac{\kappa}{a^2 H^2}. \tag{2.29}$$

The energy-momentum tensor is a conserved tensor meaning that $\nabla_\mu T^{\mu\nu} = 0$, where ∇_μ is the covariant derivative (A.4). Its zeroth component applied to the tensor of the perfect fluid (2.19) gives us the time evolution of ρ:

$$\begin{aligned} \nabla_\mu T^{\mu 0} &= 0 \\ \partial_\mu T^{\mu 0} + \Gamma^\mu_{\mu\lambda} T^{\lambda 0} + \Gamma^0_{\mu\lambda} T^{\mu\lambda} &= 0 \\ \dot{\rho} + 3H(\rho + p) &= 0, \end{aligned} \tag{2.30}$$

where we have used the Christoffel symbols for the Robertson-Walker metric (B.2).

There are three basic types of fluid that we can use to model everything in the universe in a simple fashion. First we have matter made of particles whose energy is mainly rest mass, sometimes called non-relativistic matter or dust. It is taken to be pressureless so it follows from (2.30) that:

$$\rho \propto a^{-3}. \tag{2.31}$$

Alternatively, this could be seen by noting that $\rho = \frac{E}{V}$, where E is the energy. Which for dust is just the invariant rest mass and V is the volume. As the universe expands the density will decrease with the volume, thus scaling with a^{-3}.

Next we have particles that are relativistic and thus dominated by their momentum. This abstraction simply means that they behave like electromagnetic radiation. The energy-momentum tensor of light is given by [22]:

$$T^{\mu\nu} = F^{\mu\lambda} F^{\nu}{}_{\lambda} - \frac{1}{4} g^{\mu\nu} F^{\lambda\sigma} F_{\lambda\sigma} \tag{2.32}$$

where $F^{\mu\nu}$ is the electromagnetic tensor. The trace of (2.32) is:

$$T^{\lambda}{}_{\lambda} = F^{\mu\lambda} F_{\mu\lambda} - \frac{1}{4} g^{\mu\nu} g^{\nu\mu} F^{\lambda\sigma} F_{\lambda\sigma} = 0. \tag{2.33}$$

To describe radiation as a perfect fluid we must have that (2.33) equals (2.20), which implies:

$$p = \frac{1}{3}\rho, \tag{2.34}$$

so that from (2.30) we obtain:

$$\rho \propto a^{-4}. \tag{2.35}$$

This may also be inferred by noting that besides the a^{-3} scaling due to the volume expansion there is an extra a^{-1} due to the redshift of radiation: $E \propto \lambda^{-1}$, with λ the radiation's wavelength.

The other relevant fluid is the vacuum energy associated with Einstein's cosmological constant which enabled him to theorize a static universe. Its associated energy-momentum tensor is given by [22]:

$$T^{\mu\nu} = -\rho g^{\mu\nu}. \tag{2.36}$$

Comparing this to the energy-momentum of a perfect fluid (2.19) we see that vacuum energy satisfies $p = -\rho$. This means that:

$$\rho \propto a^{0}, \tag{2.37}$$

which could not have any other scaling since it is a cosmological constant. This fluid is not a mere theoretical possibility, since observations of type Ia supernovae support the existence of an unknown kind of energy known as dark energy. Curiously, it is now dominating the energy balance of the universe and making expansion accelerate, according to Raychaudhuri equation (2.24b). All cosmological experiments are thus far consistent with dark energy being a cosmological constant [1].

All these fluids satisfy a simple relation between p and ρ so we can define a generic equation of state:

$$p = w\rho \tag{2.38}$$

where w is the proportionality constant that characterizes a particular type of fluid. This allows us to solve (2.30) for this more general case:

$$\frac{\dot{\rho}}{\rho} = -3H(1+w). \tag{2.39}$$

We ingrate this equation and obtain:

$$\rho = \rho_0 a^{-3(w+1)}, \tag{2.40}$$

where ρ_0 is the initial value of the energy density.

We will end this section by summarizing useful results for the relevant types of fluids presented above, as well as for the general case, in table 2.1.

Table 2.1: Cosmological perfect fluids. Dependence of ρ on a and of a and H on time.

fluid	w	ρ	a	H
general	w	$\propto a^{-3(1+w)}$	$\propto t^{\frac{2}{3(1+w)}}$	$\frac{2}{3(1+w)t}$
dust	0	$\propto a^{-3}$	$\propto t^{\frac{2}{3}}$	$\frac{2}{3}t^{-1}$
radiation	$\frac{1}{3}$	$\propto a^{-4}$	$\propto t^{\frac{1}{2}}$	$\frac{1}{2}t^{-1}$
cosmological constant	-1	$\propto a^{0}$	$\propto \exp\left(\pm Ht\right)$	constant

2.3 Chronicle of standard cosmology

As the universe is expanding its scale must have been zero in a finite time so an eternal universe does not quite match our empirical evidences. Recent observations estimate that the age of universe t_0 is [24]:

$$t_0 = 13.787 \pm 0.020\,\text{Gyr}. \tag{2.41}$$

Assuming the simple picture we have come to consider, we may infer from the scalings in table 2.1 that the universe must have started dominated by radiation. Followed by dust and finally by a cosmological constant. This leads us to the canonical beginning of the cosmos which is a very dense and high-temperature radiation-dominated universe, informally called the Big Bang or the initial singularity. It is remarkable that such a simple hypothesis could lead to such accurate predictions as the ones we will briefly mention below.

As the universe expands the radiation cools down and the temperature T evolves as [25]:

$$T \propto a^{-1}. \tag{2.42}$$

Considering the scaling for radiation in table 2.1 we may use temperature to index the chronology of the universe (valid during the radiation dominated epoch):

$$T(t) = T_i\left(\frac{t_0}{t}\right)^{\frac{1}{2}}, \tag{2.43}$$

where $T_i = 2.7255 \pm 0.00006\,\text{K}$ is the current temperature of the CMB [20].

When the universe is hotter then the rest mass of any standard model particle, all of them will make up the radiation bath with density ρ_{rad} [4, 22]:

$$\rho_{\text{rad}} = \frac{\pi^2}{30} g_* T^4, \tag{2.44}$$

where g_* is a combination of the relativistic degrees of freedom of the particles that make up the bath:

$$g_* = n_b + \frac{7}{8} n_f. \tag{2.45}$$

With n_b and n_f the bosonic and fermionic degrees of freedom, respectively. As the universe cools down to temperatures below the rest mass of a given particle, it will no longer constitute the primordial radiation bath. This means that g_* must decrease with time.

We will now present a brief chronology of the universe from the earliest times to the present, mentioning a few relevant highlights [15]:

- $\sim \mathbf{10^{-46}}$ s $(\mathbf{10^{18}}$ GeV): Near the Planck scale general relativity can no longer be assumed valid and a new still unknown quantum gravity theory must describe the universe at these scales.

- $\sim \mathbf{10^{-18}}$ s $- \mathbf{10^{-46}}$ s $(\mathbf{10}$ TeV $- \mathbf{10^{18}}$ GeV): These energy scales are currently out of reach for particle accelerators. As so the physics in this range is an area of open research which is forcefully speculative. This epoch is not contemplated in the standard cosmology and is commonly called the early universe. Present belief is that new physics, as for example supersymmetric and unification theories, can only be expected to be probed in the near future by looking at this epoch [26].

  At approximately 10^{16} GeV it is thought that electroweak and strong interactions unify. Cosmic inflation is also believed to happen during this epoch[2] and it is one of the most relevant phenomena happening in the early universe. Its relevance stems from the fact that it can solve troubling problems of the standard cosmology without relying much on unknown physics. In particular for this work, this is also the epoch when thermal inflation is set to happen. Both of them will be further discussed in subsequent chapters.

  Fortunately for us, below the Planck scale only electroweak and strong interactions are uncharted, general relativity is still assumed to be valid.

- $\sim \mathbf{10^{-14}}$ s $- \mathbf{10^{-18}}$ s $(\mathbf{100}$ GeV $- \mathbf{10}$ TeV): This range can be probed using current accelerators and so the standard model of particle physics seems to describe accurately particles in this regime. At this stage quarks, leptons, gauge bosons and the Higgs boson are all relativistic, making up the primordial radiation bath. Approximately at 100 GeV the electroweak phase transition occurs, below which electromagnetism and the weak interaction become distinct and the weak gauge bosons acquire mass.

- $\sim \mathbf{10^{-9}}$ s $(\mathbf{200}$ MeV): At this temperature free quarks and gluons get confined in baryons and mesons. As this happens stable baryons start being non-relativistic, and stop contributing as relativistic degrees of freedom.

[2] Empirically speaking inflation is only bounded to happen before the Big Bang nucleosynthesis so it could happen at much lower energy scales.

- $\sim \mathbf{10^{-4}}$ s $(\mathbf{1 - 2}$ MeV$)$: During this period weak interactions fall out of equilibrium. An interaction falls out of equilibrium when the relevant interaction rate Γ becomes less then the Hubble expansion rate, $\Gamma \lesssim H$ [4] – the universe expands faster than the typical time reactions take to occur. This may result in the number density of a given species becoming constant, and we say that its abundance freezes-out. During this epoch, this happens to the neutrinos that decouple from the main thermal bath. Secondly the ratio of neutrons to protons also freezes-out leading to the observed relative abundance of the primordial elements.

- $\sim \mathbf{0.01}$ s $(\mathbf{0.5}$ MeV$)$: Now at the typical rest mass of electrons, the electron-positron pairs cease being relativistic and start annihilating, resulting in photons. These in their turn make the temperature of the primordial radiation bath higher than that of the neutrinos' thermal bath. The electron-positron annihilation, besides reducing the relativistic degrees of freedom, also results in a net excess of electrons compared to their antiparticles, which must be explained by some leptogenesis process [4].

- $\sim \mathbf{1}$ s $(\mathbf{0.05}$ MeV$)$: Nuclear reactions are now able to compete with the thermal effects and the free protons and neutrons combine to form light nuclei. This phase is called primordial nucleosynthesis or Big Bang nucleosynthesis. Only light nuclei are synthesized during this epoch, heavier ones can only be created in stellar processes later in the cosmic history.

  The predictions of primordial nucleosynthesis are one of the greatest accomplishments of standard cosmology because they show that general relativity, alongside nuclear physics are able to predict the abundance of light nuclei that were set around 1 s after the Big Bang. This means that any alternative hypothetical theories for the early universe must not spoil the conditions of standard cosmology that led to the Big Bang nucleosynthesis.

- $\sim \mathbf{10^8}$ s $(\mathbf{1}$ eV$)$: This is the moment of the matter-radiation equality, when the energy density of radiation and dust are equal. This marks the beginning of the matter-dominated era.

- $\sim \mathbf{10^{12} - 10^{13}}$ s: By this time all nuclei have combined with the remaining electrons into neutral light elements. At this stage, named recombination, matter stops interacting significantly with radiation. It is said that the universe becomes transparent to the radiation bath which will eventually become the CMB measured today. The photons redshift away giving rise to an ever decreasing typical peak for the black-body radiation. Today it is in the microwave region.

  Tiny temperature perturbations in the CMB are induced by small density perturbations at the moment when radiation last interacted with matter, referred in

the literature as the last scattering surface. The cosmic microwave background is thus an excellent window into the past because its information has remained essentially untouched since recombination.

- $\sim 10^{16} - 10^{17}$ s: Structure in the universe is in the form of galaxies and clusters of galaxies seeded by small inhomogeneties in the matter density that grow due to gravitational instabilities. This is our present and currently our universe is dominated by a cosmological constant as we will show below.

We are now able to present the current cosmological paradigm, the Lambda-CDM model.

2.3.1 Lambda-CDM model

Also named concordance model, the Lambda-CDM model is the current cosmological paradigm that is on fair grounds due to its accurate predictions. It posits that general relativity is correct; the universe is expanding so it is described by a Robertson-Walker metric; the space is flat and today the dominating fluid is dark energy (a form of cosmological constant that is sometimes denoted by Λ) with cold dark matter (CDM) being the second most dominant fluid.

It turned out that regular matter comprised of electrons, protons and neutrons or their combination thereof, called baryonic matter in the literature[3], could not fully account for observations [27]. Hence cold dark matter was defined. Cold, because only non-relativistic matter would clump together appropriately [1]. Its nature is still illusive but its most defining characteristic is its low interaction rate with baryonic matter and with light, hence the reason why it still has not been detected. Together, baryonic and dark matter comprise non-relativistic matter which current observation estimate to make up 31% of our universe with cold dark matter accounting for 26% and baryonic matter for only 5%. The remaining 69% of the present universe is made of dark energy, a component that behaves like a cosmological constant [28]. This faces us with the reality that most of our universe is unknown to us (see table 2.2 for precise results).

We might wonder what is the abundance of radiation and why it is not included in this model. Presently the only relativistic particles are photons and neutrinos with densities of the same order of magnitude and similar temperature [4], corresponding to an abundance of approximately $\Omega_r \approx 10^{-4}$ [22], two orders of magnitude smaller than the abundance of baryonic matter. This is intuitive since we are ten billion years away from the matter-radiation equality. In conclusion, radiation is usually neglected as far as present densities are concerned.

[3]This component is called baryonic matter because the mass of the stable baryons is three orders of magnitude greater than that of electrons.

To complete the concordance model we indicate a recent measurement for the curvature abundance $\Omega_\kappa = 0.0007 \pm 0.0019$ [24], which indicates that our universe is flat to a great degree of precision.

As a quick note, theological and philosophical cosmologies always tried to answer what was the ultimate fate of the universe and what it meant for the end of humanity. In a simple approach using the Raychaudhuri equation (2.24b) and assuming that nothing radical happens to the energy content of the universe, dark energy will dominate in the asymptotic future:

$$\frac{\ddot{a}}{a} \approx \frac{1}{3M_p^2}\rho_\Lambda, \tag{2.46}$$

where ρ_Λ is the energy density of the dark energy. This seems to imply that the universe will expand in an accelerated fashion eternally [29].

Currently it is almost standard to consider a period of inflation in the early universe that both solves the fine-tuning problems of standard cosmology and creates the initial perturbations that lead to structure forming later in the history of the universe [1, 2, 26]. In the following chapter we go a little deeper in understanding these problems and how inflation succeeds in dealing with them.

Table 2.2: Present day abundances of the various energy components of the universe. Data taken from the Planck mission 2018 [24].

component	**abundance**
Ω_b (baryonic matter)	0.0489 ± 0.0001
Ω_c (cold dark matter)	0.2607 ± 0.0008
Ω_Λ (dark energy)	0.6889 ± 0.0056

Chapter 3

Inflation

Standard cosmology, when inspected closely describes a universe that is incredibly fined-tune. Distant regions in the night sky have never been in causal contact and nevertheless have the same CMB temperature; our universe is incredibly flat even though its matter content has been pushing it away from flatness for most of the cosmic history since the initial singularity. These are just some facets of our universe that seem highly improbable. An elegant and minimal solution is to postulate an epoch of accelerated expansion, happening right after the Big Bang, that cleanly solve all these issues without resorting to much unknown physics. Additionally, inflation can also account for the small inhomogeneities observed in the CMB, as well as accounting for the structure we observe in the universe.

3.1 A fine-tuned universe

Despite its obvious successes, like the correct prediction for the abundance of light elements, the Lambda-CDM model is plagued by some troublesome issues. Without a phenomenon such as inflation, the universe as we see it would need to evolve from a very constrained set of initial conditions. We now briefly present and discuss the arguments that expose this problem concerning the initial conditions of our universe:

- **Horizon problem :** We have assumed above, as is common practice, that the universe is homogeneous and isotropic. But are these assumption sensible? The Robertson-Walker metric is certainly a very particular solution of Einstein's equations. So why this unrelenting smoothness that we observe in the universe?

  The CMB is a good evidence of the smoothness that we postulate for our universe but it is strange that we measure the same CMB temperature in regions which were causally disconnected at the surface of last scattering[1]. We can see this by

[1] A rough estimate gives 10^5 causally disconnected regions at recombination [2, 4].

considering the comoving particle horizon [2, 3], τ:

$$\tau \equiv \int_0^t \frac{dt}{a(t)} = \int_0^a \frac{da}{a^2 H} = \int_0^a d\ln a \left(\frac{1}{aH}\right), \tag{3.1}$$

which is the maximum distance a photon can travel between 0 and t. For a comoving observer this gives the part of the universe that could be causally connected with him. We can see that the particle horizon depends on $(aH)^{-1}$, the comoving Hubble horizon. For the case of dust and radiation the comoving particle horizon grow as:

$$\tau \propto \begin{cases} a^{\frac{1}{2}} & \text{matter universe,} \\ a & \text{radiation universe.} \end{cases} \tag{3.2}$$

This means that until recombination the comoving particle horizon was monotonically increasing. The picture that standard cosmology gives us is that the particle horizon today is the greatest it ever was. In other words, disconnected regions only coming into causal contact today must happen to be at the exact same temperature we now measure in the CMB. The question that remains is how come our universe started in such a fine-tuned state to have different disconnected regions all with the same radiation temperature that we measure on the full angle range of the CMB?

- **Flatness problem :** Consider the Friedmann's equation in terms of the density parameter (2.27):

$$\Omega - 1 = \frac{\kappa}{a^2 H^2}, \tag{3.3}$$

which also depends on the comoving Hubble horizon. For a dust and a radiation dominated universe $(aH)^2 \propto t^{-\frac{2}{3}}$ and $(aH)^2 \propto t^{-1}$ respectively, so the left-hand side will grow with time. This means that in order for $|\Omega - 1|$ to be as close to 0 as it is today (with a precision of 10^{-3}) the universe must have had started unbelievably flat to still be this flat, billion years after[2]. Again, this also seems to imply a very fine-tuned universe.

We must stress that even though we called problems to the above assertions, they are not inconsistencies in the physical theory. It is more a philosophical issue that makes physicists uneasy about fine-tuned explanations of physical phenomena. It would surely by nicer to have the particular conditions of our universe to have been set by some process, rather than just postulating a very special set of initial conditions.

[2]For example, the universe must have satisfied $|\Omega - 1| \lesssim 10^{-17}$ at the Big Bang nucleosynthesis when its temperature was of the order of 0.1 MeV. Reaching the bound of $|\Omega - 1| \lesssim 10^{-63}$ at the Planck scale.

These problems ultimately stem from the fact that during standard cosmology the comoving Hubble horizon is ever increasing. This means that the particle horizon is dominated by the present comoving Hubble horizon such that the greatest portion of the universe that ever was in causal contact is the presently accessible universe. This make the solution of the problems above quite straightforward – if the comoving Hubble horizon started large at very early times and then was strongly decreased, we could solve the horizon problem and the flatness problem in one go. After that the comoving Hubble horizon would increase monotonically, as is expected in the Big Bang cosmology.

This means that presently causally disconnected regions would have been connected sometime in the past. Considering equation (3.1), this argument means that while in standard cosmology this integral gets its largest contribution from its upper limit, we are now putting forth the proposition that it gets its leading contribution from the lower limit of the integral.

For the horizon problem, if the comoving Hubble horizon had started greater then the present comoving Hubble horizon we have that the smoothness of our universe was brought about by causal physics during those earlier times and no fine-tuning is required.

For the flatness problem, an epoch where $(aH)^{-1}$ decreases makes equation (3.3) an attractor for a flat universe. If the right-hand side decreases enough then it may increase during standard cosmology and still be flat to the degree observed today.

Thus, we have exchanged a fine-tuned universe by a plausible unproved phenomenon that is called inflation [30, 31]. As it stands it may seem that we are hiding away our handicaps in the early universe but if this inflationary period were proved it would be a whole different story [32]. Furthermore, if the problems mentioned above cannot be properly solved during standard cosmology we must turn to what precedes it.

3.2 An inflationary period

As we saw in the previous section we need a period where the comoving Hubble horizon decreases. We can recast this assertion in equivalent ways to learn more about this event that would solve standard cosmology's fine-tuning problem. Mathematically, we need a decreasing Hubble horizon:

$$\frac{d}{dt}\left(\frac{1}{aH}\right) < 0. \tag{3.4}$$

As the comoving Hubble comoving horizon is simply $\dot{a}^{-1}$, we have that the above condition is equivalent to:

$$\ddot{a} > 0, \tag{3.5}$$

so during this period we must have an accelerated expansion. Now by recalling the Raychaudhuri equation (2.24b), we see that this is accomplished if the universe is dominated by a fluid that satisfies:

$$p < -\frac{1}{3}\rho. \tag{3.6}$$

In essence we need that during a period of time the universe be dominated by a fluid with negative pressure! From our list of most relevant perfect fluids in table 2.1 we immediately see that a cosmological constant-dominated universe could do the trick, as in that case we have $p = -\rho$.

We must end this section by referring that even if an inflationary epoch solves the problems stated above there must be a smooth transition from inflation to the radiation epoch that is the starting point of standard cosmology. This was the most stringent problem faced by the old inflation theory [30] which could never end but was later solved (see for example [31]). The conclusion is that the inflationary period will decrease the temperature of the universe and so we need some process that will transition a cold universe back into a hot radiation bath. This process is named reheating and may be accomplished in different ways [4, 26, 33].

We will present below the paradigmatic model of slow-roll inflation, but there exist many more classes of models for inflation [33]. For example, in warm inflation, reheating happens concurrently with inflation itself [4, 13], while in the conventional slow-roll inflation it happens at the end of the inflationary period.

3.2.1 Slow-roll inflation

In this model the inflationary period is brought about by a classical real scalar field ϕ named inflaton. Inflation is maintained by the inflaton as it slowly rolls down its potential. We start by presenting useful results concerning a classical real scalar field.

Dynamics of a classical real scalar field

The action of a real scalar field is given by [4, 22]:

$$S_\phi = \int d^4x\, \sqrt{-g}\left[-\frac{1}{2} g^{\mu\nu}\nabla_\mu\phi\nabla_\nu\phi - V(\phi)\right]. \tag{3.7}$$

From equation (2.18) the energy-momentum tensor for the real scalar field is:

$$T_{\mu\nu} = -\frac{2}{\sqrt{-g}}\frac{\delta S_\phi}{\delta g^{\mu\nu}}. \tag{3.8}$$

This means that we need to vary the action (3.7) with respect to the metric $g^{\mu\nu}$:

$$\delta S_\phi = \int d^4x \left\{ \delta\sqrt{-g}\left[-\frac{1}{2} g^{\rho\sigma}\nabla_\rho\phi\nabla_\sigma\phi - V(\phi)\right] - \frac{1}{2}\sqrt{-g}\delta g^{\mu\nu}\nabla_\mu\phi\nabla_\nu\phi \right\}, \tag{3.9}$$

using $\delta\sqrt{-g} = -\frac{1}{2}g_{\mu\nu}\sqrt{-g}\delta g^{\mu\nu}$ [22] we obtain:

$$\delta S_\phi = -\int d^4x\, \frac{\sqrt{-g}}{2}\left\{ g_{\mu\nu}\left[-\frac{1}{2}g^{\rho\sigma}\nabla_\rho\phi\nabla_\sigma\phi - V(\phi)\right] + \nabla_\mu\phi\nabla_\nu\phi\right\}\delta g^{\mu\nu}. \tag{3.10}$$

Applying the definition above (3.8), $T_{\mu\nu}$ for the real scalar field is:

$$T_{\mu\nu} = \nabla_\mu\phi\nabla_\nu\phi - \frac{1}{2}g_{\mu\nu}g^{\rho\sigma}\nabla_\rho\phi\nabla_\sigma\phi - g_{\mu\nu}V(\phi). \tag{3.11}$$

By examining the energy-momentum tensor of a perfect fluid in a comoving frame (2.19) we see that its diagonal components are:

$$\begin{aligned} T_{00} &= \rho_\phi \\ T_{ij} &= p_\phi g_{ij}. \end{aligned} \tag{3.12}$$

Comparing this to (3.11) we are able to compute the energy density and pressure associated with the real scalar field:

$$\begin{aligned} \rho_\phi &= \frac{1}{2}\dot\phi^2 + \frac{1}{2}g^{ij}\partial_i\phi\partial_j\phi + V(\phi) \\ p_\phi &= \frac{1}{3}T_{ij}g^{ij} = \frac{1}{2}\dot\phi^2 - \frac{1}{6}g^{ij}\partial_i\phi\partial_j\phi - V(\phi). \end{aligned} \tag{3.13}$$

For a flat Robertson-Walker universe[3], $g^{ij} = a^{-2}\delta^{ij}$ and we obtain:

$$\begin{aligned} \rho_\phi &= \frac{1}{2}\dot\phi^2 + \frac{1}{2}a^{-2}\partial_i\phi\partial_i\phi + V(\phi) \\ p_\phi &= \frac{1}{3}T_{ij}g^{ij} = \frac{1}{2}\dot\phi^2 - \frac{1}{6}a^{-2}\partial_i\phi\partial_i\phi - V(\phi). \end{aligned} \tag{3.14}$$

We now consider that the inflaton is homogeneous $\phi(t, \boldsymbol{x}) = \phi(t)$. The associated proportionality constant w (cf. (2.38)) satisfies:

$$w = \frac{\frac{1}{2}\dot\phi^2 - V(\phi)}{\frac{1}{2}\dot\phi^2 + V(\phi)}. \tag{3.15}$$

We now see if we have the inflaton's potential energy dominate over the kinetic term (i.e. rolls down the potential slowly enough), we will have inflation. The inflaton then behaves like a cosmological constant ($w = -1$) and it satisfies the condition for accelerated expansion (3.6).

[3]We may assume this for simplicity since inflation will rapidly dilute away any initial spatial curvature.

We finish this section by deriving the equation of motion for the homogeneous inflaton in curved space-time. This simply amounts to varying (3.7) with respect to the scalar field ϕ and set it to zero:

$$\int d^4x\sqrt{-g}\Big[- g^{\mu\nu}\nabla_\mu\delta\phi\nabla_\nu\phi - \frac{dV}{d\phi}\delta\phi\Big] = 0. \tag{3.16}$$

Using integration by parts in the first term and since the field is held fixed at infinity, we obtain:

$$\int d^4x\sqrt{-g}\left[\frac{1}{\sqrt{-g}}\nabla_\mu(\sqrt{-g}g^{\mu\nu}\nabla_\nu\phi) - \frac{dV}{d\phi}\right]\delta\phi = 0. \tag{3.17}$$

The equation of motion is:

$$\frac{1}{\sqrt{-g}}g^{\mu\nu}\nabla_\mu(\sqrt{-g}\partial_\nu\phi) - \frac{dV}{d\phi} = 0. \tag{3.18}$$

For a flat Robertson-Walker universe $\sqrt{-g} = a^3$ and keeping in mind that the field is homogeneous, we arrive at the equation of motion:

$$\ddot{\phi} + 3H\dot{\phi} + V'(\phi) = 0, \tag{3.19}$$

where we have made use of the covariant derivative of a one-form (A.3).

Additionally, the inflaton satisfies the Friedmann equation (2.24a):

$$H^2 = \frac{1}{3M_p^2}\left(\frac{1}{2}\dot{\phi}^2 + V(\phi)\right). \tag{3.20}$$

Slow-roll conditions

We saw above that an homogeneous real scalar field may behave like a cosmological constant and induce an inflationary epoch. Nonetheless, we must have that the potential energy dominates long enough for inflation to solve the cosmological problems presented in the first section.

Slow-roll inflation stands on two conditions [3, 4]:

1. The potential energy must dominate the kinetic term:

$$\frac{1}{2}\frac{\dot{\phi}^2}{V} \ll 1. \tag{3.21}$$

2. In (3.19) the acceleration term must not dominate the velocity term nor $V'(\phi)$ before the end of inflation, otherwise the first condition could not be maintained long enough:

$$\begin{aligned} \frac{|\ddot{\phi}|}{3H|\dot{\phi}|} &\ll 1, \\ \frac{|\ddot{\phi}|}{|V'(\phi)|} &\ll 1. \end{aligned} \tag{3.22}$$

These are conveniently named slow-roll conditions because they ensure that the inflaton will slowly roll down the potential $V(\phi)$. Slowly because condition 2 cannot be broken. We see that $3H\dot{\phi}$ behaves like a friction term, as this term dominates, the inflaton is prevented from accelerating.

In the slow-roll approximation the governing equations for the inflaton are:

$$\begin{aligned} \dot{\phi} &\approx -\frac{V'(\phi)}{3H}, \\ H^2 &\approx \frac{1}{3M_p^2} V(\phi). \end{aligned} \tag{3.23}$$

Using these, We now introduce the slow-roll parameters ϵ and η:

$$\begin{aligned} \epsilon &\equiv \frac{M_p^2}{2}\left(\frac{V'(\phi)}{V(\phi)}\right)^2, \\ \eta &\equiv M_p^2 \frac{V''(\phi)}{V(\phi)}. \end{aligned} \tag{3.24}$$

The introduction of M_p makes these slow-roll parameters adimensional. Using the inflaton equations of motion in the slow-roll approximation (3.23), we see that the two slow-roll conditions can be translated into conditions on the relative slop and relative curvature of the potential $V(\phi)$:

$$\begin{aligned} \epsilon &\ll 1 \\ |\eta| &\ll 1. \end{aligned} \tag{3.25}$$

In other words the potential must be appreciably flat and slopeless.

If the universe is dominated by a positive cosmological constant (as is the case of inflation) we have that the scale factor behaves like (see table 2.1):

$$a \propto \exp(Ht). \tag{3.26}$$

It is common practice to work with the number of e-folds N_e, defined as:

$$dN_e = Hdt, \tag{3.27}$$

instead of with time. Slow-roll inflation will end when the conditions (3.25) are violated, this is $\epsilon \sim |\eta| \sim 1$. Using the slow roll conditions we have for the number of e-folds:

$$N_e = \int_{t_{\text{begin}}}^{t_{\text{end}}} Hdt = \int_{\phi_{\text{begin}}}^{\phi_{\text{end}}} \frac{H}{\dot{\phi}} d\phi \simeq \frac{1}{M_p^2} \int_{\phi_{\text{end}}}^{\phi_{\text{begin}}} \frac{V}{V'} d\phi. \tag{3.28}$$

It is desirable that inflation lasts around 60 e-folds to solve the problems of standard cosmology [3], which impose conditions on the potential as well on the magnitude of the inflaton field.

Besides avoiding a fined-tuned universe, it is now widely accepted that inflation is responsible for both the curvature perturbations that lead to the anisotropies in the cosmic microwave background, and also provide the seeds for structure formation [3, 6, 10]. These are due to quantum fluctuations of the inflaton field being stretched and amplified by the accelerated expansion, then their amplitude freezing out once they become larger than the Hubble horizon. We will see in this thesis that a similar mechanism occurs for a period of thermal inflation, to which we will now turn our discussion.

Chapter 4

Thermal inflation

Inflation was originally developed to solve the horizon and flatness problems but after the inflationary theory was proposed it was noticed that it could happen in other contexts, having other cosmological effects. In this chapter, we discuss the dynamics of thermal inflation, where a scalar field behaves like a cosmological constant because it is trapped in a false vacuum state due to thermal effects.

4.1 Overview

Supersymmetry is presently a common feature of attempts at a quantum theory of gravity, such as supergravity or string theory. The most popular supergravity theories are, however, not compatible with the history of the universe presented in the above chapters – a radiation epoch preceded by inflation. They predict, in particular, an overabundance of gravitinos (the spin $3/2$ superpartner of the graviton), gauge monopoles, and various species of spin 0 particles with masses around 10^2 to 10^3 GeV called moduli. The overabundance of the gravitinos and of moduli give rise to the well-known gravitino [34] and Polonyi/moduli [6] problems, respectively. These, in their turn, spoil the predictions of standard Big Bang nucleosynthesis, rendering supersymmetry inconsistent with the standard cosmology. Although inflation dilutes these kinds of relics due to its exponential expansion, they may be regenerated during the reheating process.

A certain class of scalar fields with a very large vacuum expectation value[1] (VEV) M and an almost flat potential appears naturally in supersymmetric theories [6, 35]. Due to their flat potential, these scalar fields are commonly called flaton fields or simply flatons in the literature [6, 34, 35]. When we speak of «large» VEV and «almost flat» potential we mean this with respect to the scale of supersymmetry breaking, thought to be around 10^2 to 10^3 GeV [36]. So, for flatons, their mass defined as $|V''|^{\frac{1}{2}}$ is of this

[1] In this context the VEV is defined as the field value at the minimum of its potential.

order while M is far greater than the scale of supersymmetry breaking. This makes the curvature of the potential very small up to Planckian field values.

In certain conditions that we will discuss in this chapter, the flaton field can behave like a cosmological constant and hence start and maintain an epoch of inflation. This period is termed thermal inflation and its name will come to be meaningful in due course. In conclusion, this second round of inflation happening at a lower energy scale could then solve the gravitino and Polonyi/moduli problems and bring TeV-scale supergravity models into agreement with standard cosmology [5].

It is known that the duration of the main period of inflation should be around 50 to 60 e-folds in order to simultaneously solve the problems of standard cosmology and explain both the CMB anisotropies and the large scale structure of the universe [2, 26]. To achieve this, the potential of the inflaton at the end of the primary inflation must satisfy [37, 38]:

$$V^{\frac{1}{4}} \lesssim 10^{16}\,\text{GeV}. \tag{4.1}$$

This scale is, however, too high to solve the moduli problem [5]. This results in the moduli being promptly diluted during the main inflation period but regenerating afterwards [6]. So the limit on the potential must be lower [5]:

$$V^{\frac{1}{4}} \lesssim 10^{7}\text{ to }10^{8}\,\text{GeV}\left(\frac{\text{GeV}}{T_R}\right)^{\frac{1}{4}}, \tag{4.2}$$

where T_R is the reheating temperature. An estimate for the reheating temperature can be obtained by considering that the inflaton's energy density is almost instantaneously converted to radiation at the end of inflation. Since the flaton's energy density is dominated by the potential during inflation, we have:

$$T_R \sim \left(\frac{30}{\pi^2 g_*}V\right)^{\frac{1}{4}}. \tag{4.3}$$

Nevertheless, the true reheating temperature should be less than this since the inflaton typically interacts weakly with other particles and may therefore decay slowly compared to the Hubble time at the end of inflation. Using the upper bound (4.1), we nevertheless see that the reheating temperature is typically much higher than the GeV scale. So it is effectively hard for the first inflation epoch to solve the moduli problem [6]. So it was suggested [39] that the main period of inflation would solve the problems of standard cosmology and generate density perturbations on large scales, while a shorter second period of inflation at a lower scale may solve the moduli problem without affecting the density perturbations leading to CMB anisotropies and large scale structure [35]. In addition, during this period of thermal inflation, curvature perturbations may be generated at smaller scales then those created in the primary inflation

period. This could be relevant, for instance, to the creation of primordial black holes, to which we will turn to later in this work.

At such low scales it is difficult to have slow-roll inflation since a condition for this to happen is that $|V''(\phi)| \ll M_p^{-2}|V|$. The bound (4.2) and the estimate for T_R (4.3) give a very small upper bound on the mass of the flaton field that would be responsible for slow-roll inflation $m \lesssim 0.1\,\text{eV}$.

So during thermal inflation the flaton field is not rolling at all, it is just kept in a finite false vacuum at the origin by finite temperature effects. These effects arise because during this period the flaton field will interact with the ambient radiation bath created during reheating. The flaton acquires a thermal mass induced by the radiation bath, which creates a dip in the potential at the origin. If the flaton has had enough time to settle at that vacuum, then by (3.14) it will behave like a cosmological constant and lead to inflation, provided that flaton's potential energy dominates over the thermal bath.

The flaton will remain there until a critical temperature T_c is reached [5, 6], as the exponential expansion will reduce the thermal mass exponentially fast until it becomes comparable with the flaton's zero temperature mass. When this happens, the origin becomes a maximum and the true vacuum appears. This can only be accomplished if the zero temperature mass is negative. As the flaton evolves towards the new VEV the conditions for inflation are violated and thermal inflation ends.

We emphasize that during thermal inflation the abundance of gravitinos and of moduli fields will be diluted, rendering supergravity consistent with standard cosmology [5]. These are the main motivation for thermal inflation, requiring just 10 e-folds to dilute the moduli [6].

In summary, if the premise that an epoch of thermal inflation should occur, then there is a clear layout for the early universe:

1. Our universe begins with the initial singularity (or a suitable replacement in quantum gravity).

2. A first period of inflation takes place, creating a flat homogeneous and isotropic universe.

3. Reheating happens and leads to a radiation-dominated universe. In the process, supergravity theories predict the creation of relics that would compromise standard cosmology's predictions.

4. Thermal inflation ensues after the flaton responsible for it settles at the origin. The unwanted relics are diluted away.

5. The decay of the flaton leads to a radiation-dominated universe, which is the beginning of the Big Bang cosmology.

4.2 The flaton potential

In supersymmetric theories, the flaton arises from a complex field [6]:

$$\Phi(\boldsymbol{x}, t) = \phi(\boldsymbol{x}, t) \exp(i\theta(\boldsymbol{x}, t)), \tag{4.4}$$

as supersymmetry transforms Weyl fermions into complex scalars and vice-versa, both with two degrees of freedom [36]. Generically such fields are charged under a global $U(1)$ symmetry and so the action must be invariant under the transformation $\Phi \to \Phi \exp(i\alpha)$. Thus the potential depend on Φ only through $|\Phi| = \phi$. This, in turn, means that only one of the Φ's degrees of freedom will play a role. So for all that follows, we take the flaton to be a real scalar field ϕ.

Assuming an effective field theory that is valid up to Planck scale, the flaton potential is generically of the form [6]:

$$V(\phi) = V_0 - \frac{1}{2}m^2\phi^2 + \sum_{n=1}^{\infty} \lambda_n (2n+4)^{-1} M_p^{-2n} \phi^{2n+4}, \tag{4.5}$$

where V_0 is a constant and the couplings λ_n are assumed to be at most unity (for validity of perturbative calculations), and m is the mass of the flaton which, as said above, is of the order of the supersymmetry breaking scale.

A crucial feature of this potential is the absence of the quartic term ϕ^4, which is what makes it flat as we will see below. This is a fundamental feature of flat directions in the scalar field space of supersymmetric theories, such as the minimal supersymmetric standard model [40], that is not spoiled by the spontaneous breaking of supersymmetry. Planck-suppressed non-renormalizable terms are typical of supergravity theories, and we require only that the highest order term is positive for boundedness of the potential. The quadratic term must be negative in order for the phase transition to occur.

The flaton potential in (4.5) is not what its typically assumed when one considers spontaneous symmetry breaking in the early universe. It is more common to use an Higgs' potential [2, 26]:

$$V = \lambda\left(\phi^2 - M^2\right)^2, \tag{4.6}$$

where M is the VEV and the coupling $\lambda \sim 1$. This choice is not natural when we are dealing with a flaton field because this potential does not allow for its curvature $|V''|^{\frac{1}{2}}$ to be much less than its VEV near the origin. As can be seen in:

$$|V''(0)|^{\frac{1}{2}} = 2\lambda^{\frac{1}{2}} M. \tag{4.7}$$

Hence, this cannot correspond to a flaton field and (4.5) should be regarded as the default case instead [6, 34, 35]. One can also show that thermal inflation with a Higgs-like potential would only last for sufficiently long if the coupling λ were unnaturally small.

We assume that the flaton field interacts with the particles that make up the radiation bath. The couplings to these light degrees of freedom give a thermal mass to the flaton and thus make it acquire an effective mass $(\alpha^2 T^2 - m^2)$, such that the effective potential gains a local minimum at the origin for temperatures greater than a critical temperature T_c [35]. Below T_c the true vacuum appears at a lower potential. Thermal inflation ends as the flaton field progressed towards it. We might expect that the flaton might tunnel from the false vacuum to the true vacuum, however, as the tunneling rate is so small, we may ignore it [34].

4.2.1 Flaton thermal mass

We have mention above that the flaton is held at the origin by thermal effects. We now delve more into how this comes to be.

Before the onset of thermal inflation the flaton will be amidst other particles making up the radiation bath that dominates the universe. Let us suppose, for simplicity (but without a significant loss of generality), that the radiation bath is made up only of Dirac fermions ψ_i, to which the flaton can couple through a Yukawa coupling $-g_i \phi \bar{\psi}_i \psi_i$. These interactions will give the corrections to the flaton potential (4.5), which have the form [35, 41]:

$$V_{\text{fermions}} = -4 \times \frac{T^4}{2\pi^2} \int_0^\infty dx\, x^2 \ln \left\{ 1 + \exp \left[- \sqrt{x^2 + \frac{m_{\psi_i}^2}{T^2}} \right] \right\}. \tag{4.8}$$

Note that V_{fermions} is multiplied by 4 to account for its four degrees of freedom. In this expression, m_{ψ_i} denotes the mass of ith fermion coupled to the flaton. We suppose that the fermions in question are light enough such that the dominant contribution to their mass comes from their coupling to the flaton.

As these fermions are the constituents of the radiation bath we can simplify their contributions to the potential (4.8) by considering the high temperature limit. This yields:

$$V_{\text{fermions}} = -\frac{7\pi^2}{180} T^4 + \frac{1}{12} m_{\psi_i}^2 T^2 + \cdots, \tag{4.9}$$

The first term does not depend on the flaton field ϕ and since that its governing equation (5.5), to be presented below, only depends on the potential through $V'(\phi)$ we can safely ignore this term.

As we discussed above the fermions will acquire masses through their couplings to the flaton:

$$m_{\psi_i} = g_i \phi. \tag{4.10}$$

This amounts to adding to the overall flaton potential (4.5) the term:

$$\frac{1}{2} \alpha^2 T^2 \phi^2, \tag{4.11}$$

where we have defined α to be:

$$\alpha^2 \equiv \frac{1}{6}\sum_i g_i^2, \tag{4.12}$$

with the sum running over all the species of fermions.

All things considered this amounts to adding a thermal mass [35, 42]:

$$-m^2 \to \alpha^2 T^2 - m^2 \tag{4.13}$$

to the flaton's zero-temperature mass. Hence we define the flaton's effective mass m_{eff}:

$$m_{\text{eff}}^2 = \left(\alpha^2 T^2 - m^2\right). \tag{4.14}$$

Which is positive above the critical temperature $T_c = \frac{m}{\alpha}$ and negative below. This feature will be a fundamental characteristic of thermal inflation.

4.3 Dynamics of thermal inflation

Since during thermal inflation the flaton field is trapped at the origin with, as we will show, sub-Planckian fluctuations, we may truncate the potential at the leading non-renormalizable term, $\mathcal{O}(\phi^6)$. Adding the thermal mass discussed in the previous section, we then have for the potential of the flaton:

$$V(\phi) = V_0 + \frac{1}{2}m_{\text{eff}}^2\phi^2 + \frac{1}{6}\frac{\phi^6}{\Lambda^2}, \tag{4.15}$$

where we have defined $\Lambda = \frac{M_p}{\sqrt{\lambda}}$ which is at least M_p.

This potential has three extrema: $\phi = 0$ and $\phi^2 = \Lambda(m^2 - \alpha^2 T^2)^{\frac{1}{2}}$ (only the positive root since ϕ is real). At a temperature greater then the critical temperature $T_c = \frac{m}{\alpha}$, there is a false vacuum at the origin. When $T \approx T_c$ the thermal mass is balanced by the zero-temperature mass and the origin becomes a maximum at lower temperatures. Below the critical temperature the potential has minima for:

$$\phi = M = \pm\Lambda^{\frac{1}{2}}\left(m^2 - \alpha^2 T^2\right)^{\frac{1}{4}}, \tag{4.16}$$

which correspond to the true VEV.

Given the smallness of the observed cosmological constant, we will set the potential to zero at the VEV when $T = 0$, which yields $V_0 = \frac{1}{3}M_0^2 m^2$, where $M_0 = M(T = 0) = \pm(\Lambda m)^{\frac{1}{2}}$, i.e the VEV at zero temperature. The potential is then rewritten using the parameters that naturally describe a flaton field, its curvature m and its true VEV M_0:

$$V(\phi) = \frac{1}{3}M_0^2 m^2 + \frac{1}{2}m_{\text{eff}}^2\phi^2 + \frac{1}{6}\frac{m^2}{M_0^4}\phi^6. \tag{4.17}$$

Before thermal inflation starts the universe will be radiation-dominated with an energy density given by (2.44) and so thermal inflation begins when $\rho_{\text{rad}} \lesssim V(0)$, meaning:

$$T \lesssim \left(\frac{10}{\pi^2 g_*}\right)^{\frac{1}{4}} \sqrt{mM_0}. \tag{4.18}$$

We will then define the upper limit as the temperature at which thermal inflation starts T_i:

$$T_i = \left(\frac{10}{\pi^2 g_*}\right)^{\frac{1}{4}} \sqrt{mM_0}, \tag{4.19}$$

and:

$$T_c = \frac{m}{\alpha}, \tag{4.20}$$

will be the temperature when it ends.

Due the form of the potential (4.17) above T_c, the flaton will settle at the origin making its kinetic energy negligible [2]. Considering (3.14) we see that the flaton behaves like a cosmological constant. Note that in this case we do not require an homogeneous field to ignore the gradient terms.

During an inflationary period we have that (see table 2.1):

$$a(t) \propto \exp(Ht), \tag{4.21}$$

with H a positive constant. During thermal inflation the energy density of the universe will be dominated by the constant term in (4.17), making the Hubble parameter approximately:

$$H \approx \frac{m}{3}\frac{M_0}{M_p}, \tag{4.22}$$

where we used Friedman's equation (2.24a). This means that the temperature decreases exponentially until it reaches T_c, terminating thermal inflation. The overall behavior of the flaton potential (4.17) is represented in figure 4.1.

From the definition of the number of e-folds (3.27) and from (2.42) the duration of thermal inflation is:

$$N_e = \ln\left(\frac{T_i}{T_c}\right) \simeq \frac{1}{2}\ln\left(\frac{M_0}{m}\right) + \ln(\alpha) + \frac{1}{4}\left(\frac{10}{\pi^2 g_*}\right), \tag{4.23}$$

so thermal inflation will last approximately 10 e-folds, if $M_0 \sim 10^{14}$ GeV and $m_0 \sim 100$ GeV [5, 6, 35].

We end this section with a brief note about the parameters involved in this work. These are the effective coupling α that we assume to be in the perturbative regime

[2] The field will tend to the minimum due to the Hubble expansion an its interaction with the thermal bath.

$\alpha \lesssim 1$; g_* which is related to the fermionic relativistic degrees of freedom, for the standard model and at temperatures above the electroweak scale $g_* \sim 100$; and the two mass scales that characterize the flaton potential, m and M_0, where $M_0 \gg m$.

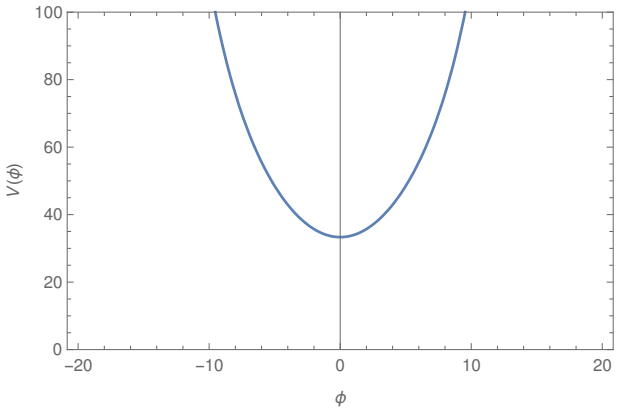

(a)

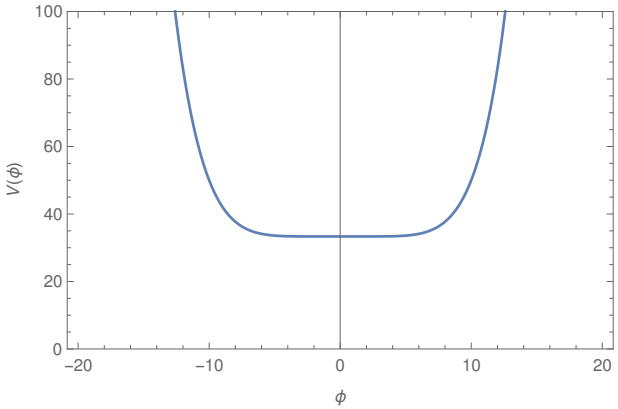

(b)

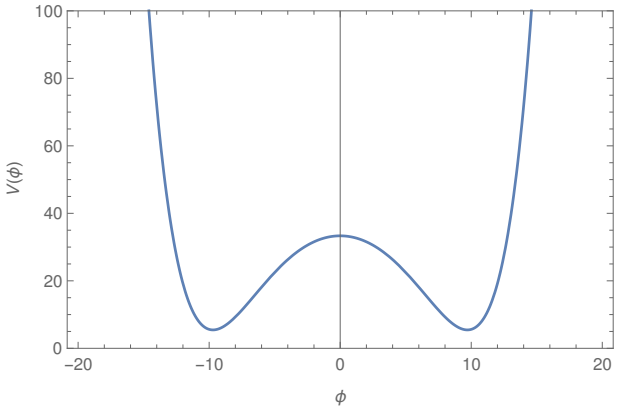

(c)

Figure 4.1: Representation of the flaton potential in equation (4.17). In regimes where it is above (panel a), at (panel b) and below (panel c) T_c. These graphs were plotted using $\alpha = 1$, $m = 1\,\text{GeV}$ and $M_0 = 10\,\text{GeV}$.

Chapter 5

Evolution of the flaton field during thermal inflation

In the previous chapter we saw how a flaton field could bring about thermal inflation by resting at the origin. In general, the flaton will not be in equilibrium with the radiation bath at the onset of thermal inflation, but it will be driven towards thermal equilibrium through its interactions with the latter. In this chapter we present and solve the differential equation that described the flaton's approach to equilibrium. As before we model the thermal bath by a set of fermions interacting via Yukawa terms with the flaton field.

5.1 Governing equation for the flaton

The Yukawa interactions between the flaton field and the fermions in the thermal bath allow the former to decay into the latter, as well as the inverse processes to occur. If, on the one hand, this results in an average dissipation of the flaton field's energy, on the other hand it also excites flaton particles in the thermal bath. These two effects are related through the well-known fluctuation-dissipation theorem and result in a stochastic dynamics for the flaton field governed by an effective Langevin equation [13, 14], which as we discuss in detail below drives the flaton field towards a thermal equilibrium configuration.

5.1.1 Thermal decay width

The flaton ϕ responsible for thermal inflation may decay into other species [42], in our case the fermions that make up the radiation bath. At finite temperature, for modes of physical three-momentum p, the flaton decay width into fermions is given

by [43]:

$$\Gamma_\phi(p) = \frac{3m_{\text{eff}}^2\alpha^2}{4\pi\omega_p}\left\{1 + \frac{2T}{p}\ln\left[\frac{1+\exp(-\frac{\omega_+}{T})}{1+\exp(-\frac{\omega_-}{T})}\right]\right\} \tag{5.1}$$

where $\omega_p = \sqrt{p^2 + m_{\text{eff}}^2}$ and $\omega_\pm = \frac{|\omega_p \pm p|}{2}$, with p being the absolute value of the three-momentum $\boldsymbol{p}$. Note that this expression neglects the mass of the fermions, which is a sufficiently good approximation since, as we will obtain a posteriori, $g\sqrt{\langle\phi^2\rangle} \lesssim T$ for perturbative couplings.

If we consider modes with $p \lesssim T$ we may preforming a Maclaurin expansion with respect to $\frac{p}{T}$ and obtain:

$$\Gamma_\phi \approx \frac{3m_{\text{eff}}^2\alpha^2}{4\pi\omega_p}\left[1 - \frac{2}{1+\exp\left(\frac{\omega_p}{2T}\right)}\right] = \frac{3m_{\text{eff}}^2\alpha^2}{4\pi\omega_p}\frac{\exp\left(\frac{\omega_p}{2T}\right)-1}{\exp\left(\frac{\omega_p}{2T}\right)+1}. \tag{5.2}$$

For perturbative couplings $m_{\text{eff}} \lesssim T$, which means that $\omega_p \lesssim T$. Hence, let us consider $\frac{\omega_p}{T}$ small and expand to first order:

$$\Gamma_\phi \approx \frac{3m_{\text{eff}}^2\alpha^2}{16\pi T}. \tag{5.3}$$

We now define the relative error ϵ_r between a function f and its approximation f_{approx} as:

$$\epsilon_r(f) \equiv \frac{|f - f_{\text{approx}}|}{f}. \tag{5.4}$$

We plot the relative error for the case of Γ_ϕ (5.1) and its approximation (5.3), in figure 5.1. We will thus safely use the approximation (5.3) in the rest of our work, even up to $p \sim T$. Note that both the approximated and the exact result agree at T_c, where they both vanish.

5.1.2 Langevin-like equation

The flaton ϕ is a real scalar field which is out of equilibrium by hypothesis. In a flat Robertson-Walker universe the flaton field satisfies a Langevin-like equation [13, 14, 42]:

$$\ddot{\phi} + (3H + \Gamma_\phi)\dot{\phi} - a^{-2}(t)\nabla^2\phi + V'(\phi) = \xi, \tag{5.5}$$

The Langevin equation includes, besides the average dissipative term Γ_ϕ, a Gaussian white noise term ξ. Both terms being a consequence of the interactions between the field and the thermal bath. While a rigorous derivation of this equation using non-equilibrium thermal field theory techniques is outside the scope of this thesis, we mention that this is analogous to, for instance, the Brownian motion of a particle in a gas. Where collisions with the gas particles induce an average friction in the particle's

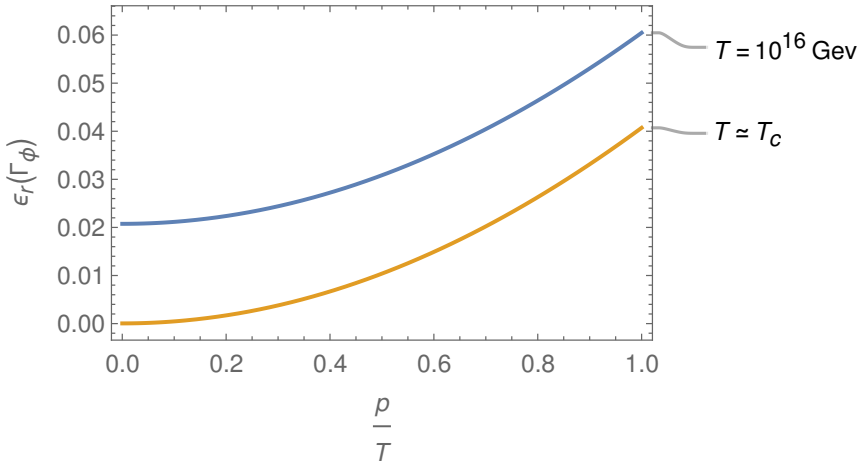

Figure 5.1: Relative error between the flaton decay width (5.1) and the approximation (5.3) up to $p = T$. For $T = 10^{16}$ GeV the maximum error is 6%, while very close to T_c it reaches 4%. To plot this graph we used $\alpha = 1$ and $m = 1$ GeV.

motion as well as random fluctuations. The average friction will reduce the particle's velocity while the random fluctuations will not let the velocity fall to zero. The net result is that the particle will tend to be in a state of equilibrium with its surroundings.

The same happens with the flaton, it will evolve towards thermal equilibrium with the ambient radiation bath. The dissipative term and the noise term are related via the fluctuation-dissipation theorem, which for the flaton field is reflected in the two-point correlator for the noise (in Fourier space) [13, 42]:

$$\langle \xi_k(t_1)\xi_{k'}(t_2)\rangle = 2\Gamma_\phi(k)T\frac{(2\pi)^3}{a^3}\delta^3(\boldsymbol{k}+\boldsymbol{k'})\delta(t_1-t_2). \tag{5.6}$$

The noise is termed white because it is completely random, i.e there is no correlation between any length nor time scales. We remark that the noise term has zero average $\langle\xi\rangle = 0$, so it only affects the evolution of field fluctuations about its average value. Note also that the noise term can only be considered Gaussian and white for distances beyond its correlation length, i.e $(\pi T)^{-1}$, or roughly, for momentum modes below the temperature of the thermal bath [34].

5.2 Flaton's equation during thermal inflation

The flaton will have the potential (4.17) described in chapter 4. The Langevin-like equation for the flaton then reads:

$$\ddot{\phi} + (3H + \Gamma_\phi)\dot{\phi} - a^{-2}(t)\nabla^2\phi + m_{\text{eff}}^2\phi + \frac{m^2}{M_0^4}\phi^5 = \xi. \tag{5.7}$$

We will discard the last term because, during thermal inflation, the flaton is settled at the origin so $\phi \ll M_p$. So we effectively must solve:

$$\ddot{\phi} + (3H + \Gamma_\phi)\dot{\phi} - a^{-2}(t)\nabla^2\phi + m_{\text{eff}}^2\phi = \xi. \tag{5.8}$$

Let us simplify the problem by considering the Fourier transform (1.1) of ϕ and ξ. This way we can just solve an ordinary differential equation:

$$\ddot{\phi}_k + (3H + \Gamma_\phi)\dot{\phi}_k + a^{-2}(t)k^2\phi_k + m_{\text{eff}}^2\phi_k = \xi_k. \tag{5.9}$$

We define the total energy of a mode ω_k as:

$$\omega_k^2 \equiv a^{-2}k^2 + m_{\text{eff}}^2. \tag{5.10}$$

The real variable k used in the Fourier transform is the comoving momentum, related to the physical momentum p as $p = a^{-1}k$. This finally gives:

$$\ddot{\phi}_k + (3H + \Gamma_\phi)\dot{\phi}_k + \omega_k^2\phi_k = \xi_k. \tag{5.11}$$

This differential equation depends on the Hubble parameter (4.22) and on the approximated decay width (5.3), which we rewrite here for convenience:

$$\begin{aligned} H &\simeq \frac{m}{3}\frac{M_0}{M_p}, \\ \Gamma_\phi &\approx \frac{3m_{\text{eff}}^2\alpha^2}{16\pi T}. \end{aligned} \tag{5.12}$$

The differential equation for the flaton (5.11) is a non-homogeneous second order linear ordinary differential equation that we will solve using the method of Green's functions [44, 45, 46]. But first we shall change to a variable which puts the above equation into a more amenable form. Remembering that $T \propto a^{-1}$ and setting $a(T_i) = 1$ we have:

$$T = T_i \exp(-Ht). \tag{5.13}$$

This allows us to expand all the terms in (5.11) to obtain:

$$\begin{aligned} \ddot{\phi}_k + \left(3H + \frac{3\alpha^4}{16\pi}T_i\exp(-Ht) - \frac{3\alpha^2 m^2}{16\pi T_i}\exp(Ht)\right)\dot{\phi}_k \\ + \left[(k^2 + \alpha^2 T_i^2)\exp(-2Ht) - m^2\right]\phi_k = \xi_k. \end{aligned} \tag{5.14}$$

We change the independent variable to:

$$z(t) \equiv z_i \exp(-Ht), \tag{5.15}$$

with $z_i = H^{-1}\sqrt{k^2 + \alpha^2 T_i^2}$.

Under this change the field time derivatives become:

$$\begin{aligned} \dot{\phi}_k &\to -zH\phi_k' \\ \ddot{\phi}_k &\to H^2(z^2\phi_k'' + z\phi_k'), \end{aligned} \tag{5.16}$$

where ϕ_k' denotes the derivative of the field modes with respect to z. The previous equation (5.14) becomes:

$$\begin{aligned} \phi_k'' + \phi_k'\left(-2z^{-1} - \frac{3\alpha^4}{16\pi}\frac{T_i}{\sqrt{k^2+\alpha^2T_i^2}} + \frac{3\alpha^2}{16\pi}\frac{m^2}{H^2}\frac{\sqrt{k^2+\alpha^2T_i^2}}{T_i}z^{-2}\right) \\ + \phi_k\left(1 - \frac{m^2}{H^2}z^{-2}\right) = \frac{\xi_k}{z^2H^2}. \end{aligned} \tag{5.17}$$

This equation does not have an analytical solution so we must make some sensible approximation.

5.2.1 Analysis of the differential equation

Simplifying (5.17) boils down to determining when the effective mass is dominated by the thermal mass or the zero temperature mass. As well as checking if the Hubble expansion dominates over the decay width or the other way around.

We are considering temperatures between an initial temperature T_i and a critical temperature T_c obtained when the thermal mass equals the zero temperature mass m. So we should have a regime when the thermal mass αT dominates and when it is comparable to m, meaning that the effective mass is close to zero. In figure 5.2 we can see that the effective mass is well approximated by the thermal mass during practically all of thermal inflation.

By referring to equations (4.22) and (5.3) we see that:

$$\frac{\Gamma_\phi}{3H} \sim \frac{m_{\text{eff}}^2\alpha^2}{mT}\frac{M_p}{M_0} \tag{5.18}$$

which at the beginning of thermal inflation is:

$$\frac{\Gamma_\phi}{3H} \sim \alpha^4\sqrt{\frac{M_0}{m}}\frac{M_p}{M_0}, \tag{5.19}$$

using equation (4.19) for the thermal inflation's initial temperature. As the hierarchy between m and M_0 is large and M_0 can be at most M_p we have that the ratio above is large during virtually all of thermal inflation (see figure 5.3), except if the effective coupling α is extremely suppressed, a fine-tuned regime that is not very interesting to our analysis.

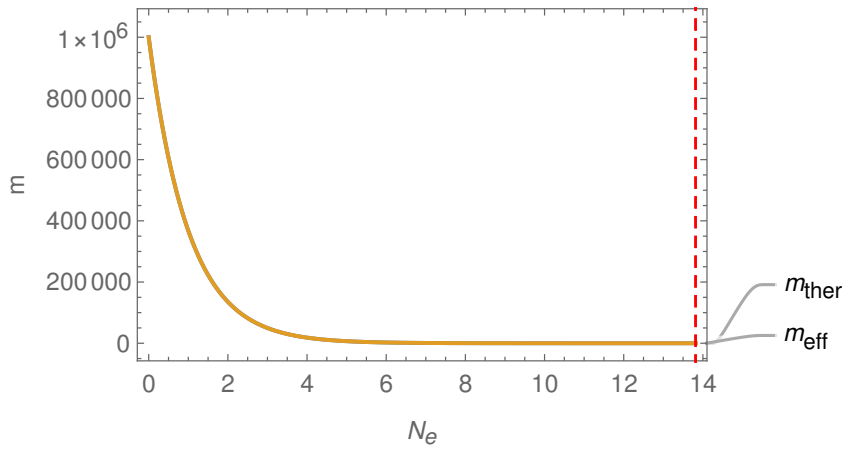

Figure 5.2: Comparison between the effective mass m_{eff} (4.14) and the thermal mass $m_{\text{ther}} = \alpha T$. The x-axis gives the number of e-folds of expansion from the onset of thermal inflation. The dashed red line represents the end of thermal inflation. The overall behavior does not depend on the hierarchy between m and M_0. This graph was plotted using $m = 1\,\text{GeV}$, $\alpha = 1$ and $M_0 = 10^{12}\,\text{GeV}$.

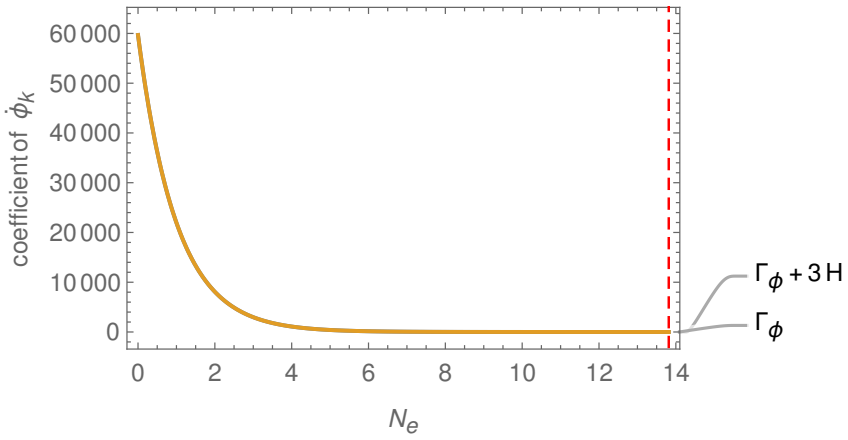

Figure 5.3: Comparison between the full coefficient of $\dot{\phi}_k$ in (5.11), $3H + \Gamma_\phi$ and just Γ_ϕ. We used the approximated form for Γ_ϕ, (5.3). The x-axis gives the number of e-folds of expansion from the onset of thermal inflation. The dashed red line represents the end of thermal inflation. This graph was plotted using $m = 1\,\text{GeV}$, $\alpha = 1$ and $M_0 = 10^{12}\,\text{GeV}$.

We thus conclude that there is a clear simplification that is neglecting the Hubble friction and ignoring the flaton's zero-temperature mass m. Throughout the rest of this work we will thus consider that $m_{\text{eff}} = \alpha T$ and that the flaton field only decays

through Γ_ϕ. This amounts to setting $m = 0$ and $H = 0$ in equation (5.14):

$$\ddot{\phi}_k + \frac{3\alpha^4}{16\pi} T_i \exp(-Ht)\dot{\phi}_k + (k^2 + \alpha^2 T_i^2)\exp(-2Ht)\phi_k = \xi_k. \tag{5.20}$$

or with respect to z (5.15):

$$\phi_k'' + \phi_k'\left(z^{-1} - A_k\right) + \phi_k = \frac{\xi_k}{z^2 H^2} \tag{5.21}$$

where we have defined:

$$A_k \equiv \frac{3\alpha^4}{16\pi} \frac{T_i}{\sqrt{k^2 + \alpha^2 T_i^2}} = \frac{3\alpha^4}{16\pi} \frac{T}{\omega_k}. \tag{5.22}$$

This quantity is small up to $k \sim T_i$ as can be seen in figure 5.4.

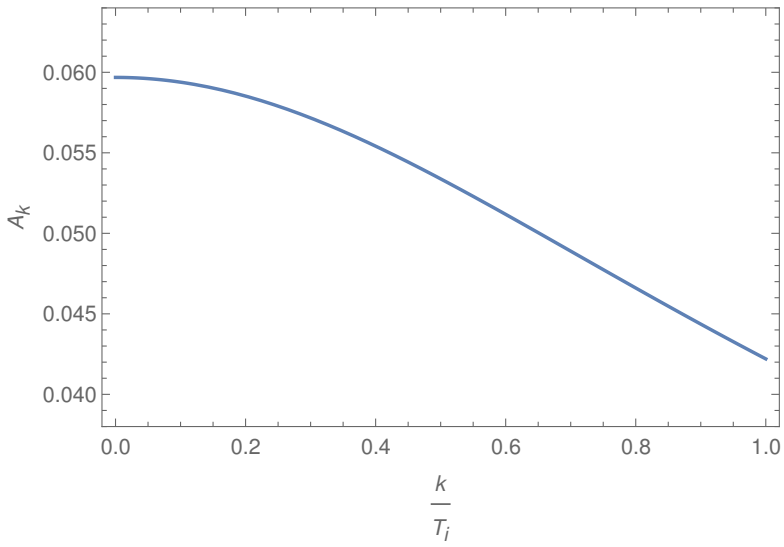

Figure 5.4: A_k as a function of $\frac{k}{T_i}$ from $k = 0$ to $k = T_i$. This graph was plotted using $\alpha = 1$.

5.3 General solution using Green's function method

The equation (5.21) is a particular example of a general second-order, linear ordinary differential equation:

$$y''(x) + p(x)y'(x) + q(x)y(x) = r(x), \tag{5.23}$$

where $p(x)$, $q(x)$ and $r(x)$ are continuous functions on the interval where the differential equation is defined. Only in this section we will take the prime $'$ to denote $\frac{d}{dx}$.

Its general solution is of the form [44, 47]:

$$y(x) = Ay_1(x) + By_2(x) + y_p(x), \tag{5.24}$$

where $\{y_1, y_2\}$ are the independent solutions of the associated homogeneous equation:

$$y''(x) + p(x)y'(x) + q(x)y(x) = 0, \tag{5.25}$$

and y_p is a particular solution of (5.23). The constants A and B are set, in our case, by initial conditions on the function $y(x)$.

For such an initial-value problem the particular solution y_p can have the form [44, 45]:

$$y_p(x) = \int_{x_0}^{x} dy\, G_s(x, y)r(y), \tag{5.26}$$

where x_0 is the initial point and:

$$G_s(x, y) = \frac{y_1(y)y_2(x) - y_1(x)y_2(y)}{W(y)}. \tag{5.27}$$

Where $W(y)$ represents the Wronskian associated with the homogeneous solutions, $W(x) \equiv y_1(x)y_2'(x) - y_1'(x)y_2(x)$. The function G_s is called the single-point Green function and has the properties: (a) is a solution of the homogeneous equation (5.25); (b) $G_s(y, y) = 0$; (c) $\frac{dG(y,y)}{dx} = 1$. This makes:

$$y_p(x_0) = y_p'(x_0) = 0, \tag{5.28}$$

so that the particular solution does not interfere with the homogeneous solutions at the initial point. This means that the homogeneous solutions alone set the values of the constants A and B through:

$$\begin{aligned} y(x_0) &= Ay_1(x_0) + By_2(x_0), \\ y'(x_0) &= Ay_1'(x_0) + By_2'(x_0). \end{aligned} \tag{5.29}$$

5.3.1 The homogeneous solutions

In light of what was exposed, we need first to solve the homogeneous form of equation (5.21):

$$\phi_k'' + \left(z^{-1} - A_k\right)\phi_k' + \phi_k = 0. \tag{5.30}$$

This equality is a form of the general confluent hypergeometric equation [48, 49] and can be replicated by setting in reference [48]:

$$\begin{aligned} A &= 0, \\ b &= 1, \\ a &= \frac{1}{2}\left(1 - \frac{A_k}{\sqrt{A_k^2 - 4}}\right), \\ h(z) &= z\sqrt{A_k^2 - 4}, \\ f(z) &= \frac{z}{2}\left(\sqrt{A_k^2 - 4} - A_k\right). \end{aligned} \tag{5.31}$$

The homogeneous solutions for the field modes are then:

$$\begin{aligned} m_k &= \exp\left[-\frac{z}{2}\left(\sqrt{A_k^2 - 4} - A_k\right)\right] M\left(\frac{1}{2}\left(1 - \frac{A_k}{\sqrt{A_k^2 - 4}}\right), 1, z\sqrt{A_k^2 - 4}\right), \\ u_k &= \exp\left[-\frac{z}{2}\left(\sqrt{A_k^2 - 4} - A_k\right)\right] U\left(\frac{1}{2}\left(1 - \frac{A_k}{\sqrt{A_k^2 - 4}}\right), 1, z\sqrt{A_k^2 - 4}\right), \end{aligned} \tag{5.32}$$

where $M(a, b, h(z))$ and $U(a, b, h(z))$ are the independent Kummer functions [46, 48].

Let us check the magnitude of A_k. Consider that the momentum is a fraction r of T_i up to unity. Then A_k reads:

$$A_k = \frac{3\alpha^4}{16\pi}\frac{1}{\sqrt{r^2 + \alpha^2}}, \tag{5.33}$$

which is very small even for strong couplings $\alpha \sim 1$, even for low momenta (see also figure 5.4).

We will thus ignore A_k in the arguments of the Kummer functions but keep them up to linear order in the exponential part:

$$\begin{aligned} m_k &= \exp(-iz)\exp\left(\frac{A_k z}{2}\right) M\left(\frac{1}{2}, 1, 2iz\right), \\ u_k &= \exp(-iz)\exp\left(\frac{A_k z}{2}\right) U\left(\frac{1}{2}, 1, 2iz\right), \end{aligned} \tag{5.34}$$

this will yield a fairly good approximation to the complete solution (5.32) as we will soon show.

We can exploit the fact that z is large throughout thermal inflation to write the Kummer functions in terms of elementary functions. We first show this claim. Consider again that k is a fraction r of T_i. Then z_i reads:

$$z_i = \frac{T_i\sqrt{r^2 + \alpha^2}}{H} \sim \frac{M_p}{\sqrt{M_0 m}}\sqrt{r^2 + \alpha^2}, \tag{5.35}$$

which is undoubtedly large, as $\sqrt{M_0 m}$ could never be of the scale of M_p without violating the definition of a flaton field. So we can expand the Kummer functions as in [48]:

$$\begin{aligned} M\left(\frac{1}{2}, 1, 2iz\right) &\approx \frac{i}{\sqrt{\pi}}(2iz)^{-\frac{1}{2}} + \frac{1}{\sqrt{\pi}}\exp(2iz)(2iz)^{-\frac{1}{2}}, \\ U\left(\frac{1}{2}, 1, 2iz\right) &\approx (2iz)^{-\frac{1}{2}}. \end{aligned} \tag{5.36}$$

By looking at the expansions we can see that they are not completely linearly independent, M contains U. So we will ignore the first term of M and also neglect any prefactors not depending on z as initial conditions are already set by A and B (cf. (5.24)):

$$\begin{aligned} M\left(\frac{1}{2}, 1, 2iz\right) &\approx \exp(2iz)(2iz)^{-\frac{1}{2}}, \\ U\left(\frac{1}{2}, 1, 2iz\right) &\approx (2iz)^{-\frac{1}{2}}. \end{aligned} \tag{5.37}$$

Our approximate set of homogeneous solutions is then:

$$\begin{aligned} m_k &= \exp(iz)\exp\left(\frac{A_k z}{2}\right)(2iz)^{-\frac{1}{2}}, \\ u_k &= \exp(-iz)\exp\left(\frac{A_k z}{2}\right)(2iz)^{-\frac{1}{2}}. \end{aligned} \tag{5.38}$$

The overall behavior of the approximate solutions (5.38) is given in figure 5.5 and they compare well to the complete solutions. Bare in mind that $z \propto \exp(-Ht)$ so z is decreases with time. Even though a specific solution will depend on the initial conditions we can safely conclude that the field will be exponentially damped during thermal inflation. Recall that we neglected m in this approximation so it is consistent that our homogeneous solution is a continuous damping of the field modes towards the origin.

5.3.2 Particular solution

We now turn our attention to the particular solution of (5.21). From (5.26), we see that:

$$\phi_k^{(p)}(z) = H^{-2}\int_{z_i}^{z} ds\, s^{-2} G_s(z,s)\xi_k(s). \tag{5.39}$$

The single point Green function is given by:

$$G_s(z,s) = \frac{m_k(s)u_k(z) - m_k(z)u_k(s)}{W(s)}. \tag{5.40}$$

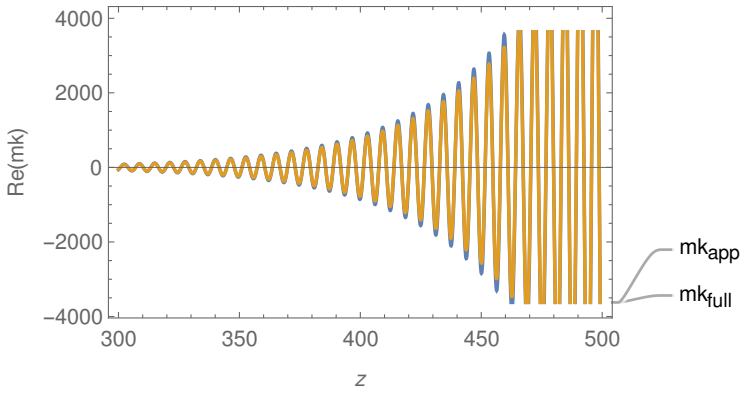

(a)

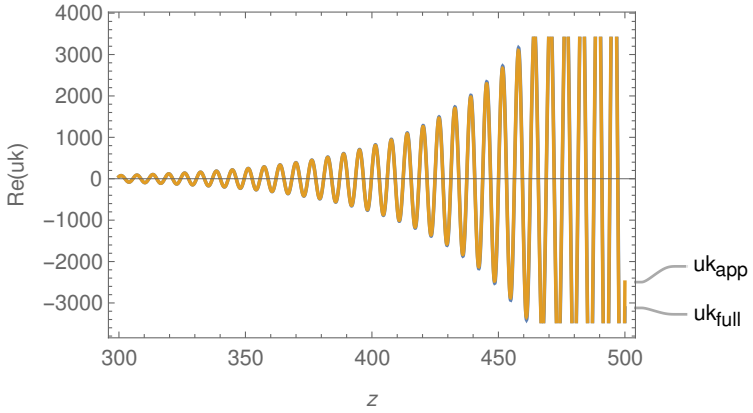

(b)

Figure 5.5: Homogeneous solutions of equation (5.21). The approximated solutions $m_{k\text{app}}$ and $u_{k\text{app}}$ (5.38) are compared with the full solutions $m_{k\text{full}}$ and $u_{k\text{full}}$ (5.32). In panel (a) we represent the real part of $m_k(z)$ and in panel (b) we represent the real part of $u_k(z)$. We used $A_k = 0.05$ to plot these graphs.

The Wronskian is the one associated with $\{m_k, u_k\}$ and has the simple form:

$$W(m_k, u_k)(s) = -\frac{\exp(A_k s)}{s}, \tag{5.41}$$

so that single-point Green function is:

$$G_s(z,s) = \left(\frac{s}{z}\right)^{\frac{1}{2}} \exp\left[\frac{A_k}{2}(z-s)\right] \sin(z-s). \tag{5.42}$$

We can finally write the particular solution of (5.21):

$$\phi_k^{(p)}(z) = H^{-2} z^{-\frac{1}{2}} \int_{z_i}^{z} ds\, s^{-\frac{3}{2}} \exp\left[\frac{A_k}{2}(z-s)\right] \sin(z-s)\xi_k(s). \tag{5.43}$$

5.3.3 Comment on the reality of the solution

What we have done so far means that the most general expression for the field modes ϕ_k is given by:

$$\phi_k(z) = Am_k(z) + Bu_k(z) + \phi_k^{(p)}(z). \tag{5.44}$$

These are the Fourier modes of a real scalar field ϕ and are related by:

$$\phi(t, \boldsymbol{x}) = \int \frac{d^3k}{(2\pi)^3}\, \phi_k(t) \exp(i\boldsymbol{k}\cdot\boldsymbol{x}), \tag{5.45}$$

and its complex conjugate is:

$$\begin{aligned} \phi^* &= \int \frac{d^3k}{(2\pi)^3}\, \phi_k^* \exp(-i\boldsymbol{k}\cdot\boldsymbol{x}) \\ &= \int \frac{d^3k}{(2\pi)^3}\, \phi_{-k}^* \exp(i\boldsymbol{k}\cdot\boldsymbol{x}), \end{aligned} \tag{5.46}$$

where in the last line we have changed the dummy variable from $k \to -k$.

The flaton field ϕ is real as such $\phi = \phi^*$. For its modes this translates into:

$$\phi_k = \phi_{-k}^*. \tag{5.47}$$

The complete flaton solution depends on k only trough k^2 in z and A_k. This means that the field modes must be real. As we will explain more thoroughly below the homogeneous part of the solution will tend to zero (both its real and imaginary parts). A quick look at the particular solution (5.43) tells us that it is also real and we can safely proceed, confident in the coherence of our results.

Chapter 6

Curvature perturbations

Having determined the behavior of the flaton during thermal inflation, we may now compute the power spectrum of the curvature perturbation. We begin by defining perturbations and see how we can bypass the arbitrariness introduced by the gauge-invariance of general relativity. After that we obtain the maximum value that the power spectrum can attain during thermal inflation on super-horizon scales and compare it with its quantum analog calculated in [10].

6.1 Gauge-invariant perturbations

In general the perturbation $\delta f(t, \boldsymbol{x})$ of a function $f(t, \boldsymbol{x})$ about its average value is defined as [3, 10]:

$$\delta f(t, \boldsymbol{x}) \equiv f(t, \boldsymbol{x}) - \langle f(t, \boldsymbol{x}) \rangle \,, \tag{6.1}$$

where the brackets $\langle . \rangle$ denotes an average. In particular the metric $g_{\mu\nu}$ and the energy density ρ perturbations are:

$$\begin{aligned} \delta g_{\mu\nu}(t, \boldsymbol{x}) &= g_{\mu\nu}(t, \boldsymbol{x}) - \langle g_{\mu\nu}(t, \boldsymbol{x}) \rangle \,, \\ \delta \rho(t, \boldsymbol{x}) &= \rho(t, \boldsymbol{x}) - \langle \rho(t, \boldsymbol{x}) \rangle \,. \end{aligned} \tag{6.2}$$

The complete Robertson-Walker metric can be decomposed into independent scalar, vectorial and tensorial components [3]:

$$\begin{aligned} ds^2 &= g_{\mu\nu} dx^\mu dx^\nu \\ &= -(1 - 2\Phi) dt^2 + 2aB_i dx^i dt + a^2[(1 - 2\Psi)\delta_{ij} + E_{ij}] dx^i dx^j, \end{aligned} \tag{6.3}$$

where Φ and Ψ are scalar perturbations. While B_i and E_{ij} are vectorial and tensorial perturbations, respectively.

As general relativity is a diffeomorphism invariant theory in the sense that many coordinates systems could be used to describe the same physical state [22, 23], there

is a inherent ambiguity in the definition of perturbations. By a clever choice of coordinates we can for example make fictitious perturbations appear or nullify physical perturbations [3]. To overcome this difficulty we must consider simultaneously matter and metric perturbations and construct gauge-invariant quantities.

In particular, we will be interested in the gauge-invariant curvature perturbation on uniform-density hypersurfaces[1] [3, 10]:

$$\zeta = \Psi + \frac{H}{\langle\dot{\rho}\rangle}\delta\rho, \tag{6.4}$$

which in the flat gauge ($\Psi = 0$) takes the simpler form:

$$\zeta = \frac{H}{\langle\dot{\rho}\rangle}\delta\rho. \tag{6.5}$$

The curvature perturbation ζ has the remarkable property that it remains constant for super-horizon modes if the perturbations are adiabatic [3]. Super-horizon modes are defined with respect to the comoving horizon, this is $(aH)^{-1}$, which gives the maximum scale for which there can be any causality with a comoving observer. As the units of momentum are (length)$^{-1}$ we see that super-horizon modes, $k < aH$, will be outside the Hubble horizon while sub-horizon modes, $k > aH$, will be inside the horizon.

An important statistical observable is the power spectrum of ζ given by [10] [2]:

$$\mathcal{P}_\zeta(k) = \frac{k^3}{2\pi^2}\int d^3x\ \exp(-i\boldsymbol{k}\cdot\boldsymbol{x})\left\langle\zeta(0)\zeta(\boldsymbol{x})\right\rangle. \tag{6.6}$$

This is just the dimensionless Fourier transform of the correlation between the curvature perturbation at distinct points.

6.2 Curvature perturbations from thermal inflation

The total energy density of the universe ρ, during thermal inflation, is given by the sum of the contributions from the flaton field and from the radiation bath:

$$\rho = \rho_\phi + \rho_{\text{rad}} = \frac{\pi^2}{30}g_*T^4 + V(\phi) + \frac{1}{2}\dot{\phi}^2 + \frac{1}{2}a^{-2}(t)\partial_i\phi\partial_i\phi, \tag{6.7}$$

where $V(\phi)$ is the potential that we have studied in chapter 4 given by (4.17). We have ignored the kinetic and gradient terms so far because the energy density of the

[1] In [3] ζ has an overall minus sign but we defined in accordance with [10] as the power spectrum of both definitions coincide in a flat gauge.

[2] Note that our definition of the Fourier transform has the opposite sign in the exponential comapred to the definition implied in [10].

universe is effectively dominated by $V(\phi)$ through its constant term $\frac{1}{3}m^2M_0^2$. But as it happens that the curvature perturbations does not depend on it, we will take all intervening terms ignoring just the non-renormalizable one for the reasons already mentioned. We are then left with:

$$\rho = \rho_\phi + \rho_{\text{rad}} = \frac{\pi^2}{30}g_* T^4 + \frac{1}{3}m^2M_0^2 + \frac{1}{2}\alpha^2T^2\phi^2 + \frac{1}{2}\dot{\phi}^2 + \frac{1}{2}a^{-2}\partial_i\phi\partial_i\phi. \tag{6.8}$$

The average energy density is thus:

$$\langle\rho\rangle \simeq \frac{\pi^2}{30}g_* T^4 + \frac{1}{3}M_0^2m^2 + \frac{1}{2}\alpha^2T^2\langle\phi^2\rangle + \frac{1}{2}\langle\dot{\phi}^2\rangle + \frac{1}{2}a^{-2}\langle\partial_i\phi\partial_i\phi\rangle\,. \tag{6.9}$$

Computing the perturbation using the definition (6.1) we get:

$$\delta\rho \simeq \frac{1}{2}\alpha^2T^2\delta(\phi^2) + \frac{1}{2}\delta(\dot{\phi}^2) + \frac{1}{2}a^{-2}\delta(\partial_i\phi\partial_i\phi). \tag{6.10}$$

6.2.1 The flaton field as a Gaussian variable

To ultimately compute the power spectrum $\mathcal{P}_\zeta$, (6.6), we will need the three variances $\langle\phi^2\rangle$, $\langle\dot{\phi}^2\rangle$ and $\langle\partial_i\phi\partial_i\phi\rangle$. This will depend indirectly on the stochastic nature that the field modes ϕ_k inherited from the noise terms ξ_k (cf. (5.39)). In particular the noise is Gaussian meaning that it only depends on its average and its variance. Its average is zero and its variance is given by the fluctuation-dissipation relation (5.6). The stochastic nature of the thermal bath that makes the flaton approach thermal equilibrium effectively turns the field and its derivatives into stochastic variables.

We start by looking at the field modes, the average of ϕ_k is:

$$\langle\phi_k\rangle(z) = Am_k(z) + Bu_k(z), \tag{6.11}$$

which is just a linear combination of the homogeneous solutions. This will of course depend on the initial conditions, but since both solutions are exponentially damped by the field's decay, as well as (sub-dominantly) by Hubble expansion, they quickly reach $\langle\phi_k\rangle = 0$ for all relevant modes.

The variance of the field modes is [50]:

$$\langle\phi_k\phi_{k'}\rangle = \langle(\phi_k - \langle\phi_k\rangle)\phi_{k'} - \langle\phi_{k'}\rangle)\rangle = \langle{\phi_k}^{(p)}{\phi_{k'}}^{(p)}\rangle\,, \tag{6.12}$$

as it follows from (6.11). So only the particular solution (5.43) contributes to the variance of the field modes.

Substituting the particular solution in the above equation, we have:

$$\begin{aligned}\langle\phi_k(z_1)\phi_{k'}(z_2)\rangle = H^{-4}z_1^{-\frac{1}{2}}z_2^{-\frac{1}{2}}\int_{z_i}^{z_1}ds_1\int_{z_i}^{z_2}ds_2\, s_1^{-\frac{3}{2}}s_2^{-\frac{3}{2}}\\ \times\exp\left[\frac{A_k}{2}(z_1-s_1)\right]\exp\left[\frac{A_{k'}}{2}(z_2-s_2)\right]\\ \times\sin(z_1-s_1)\sin(z_2-s_2)\langle\xi_k(s_1)\xi_{k'}(s_2)\rangle\,.\end{aligned} \tag{6.13}$$

We must now consider the result for the variance of the noise modes in our auxiliary variable z (C.6):

$$\langle \xi_k(z_1)\xi_{k'}(z_2)\rangle = 2Hz_1\Gamma_\phi(z_1)T(z_1)\frac{(2\pi)^3}{a^3(z_1)}\delta^3(\boldsymbol{k}+\boldsymbol{k}')\delta(z_1-z_2). \tag{6.14}$$

When applied to (6.13), this expression contains $\delta(s_1 - s_2)$ so the variance is only non-zero if $s_1 = s_2 = s$. For this to happen the integral which integrates the delta function must always be the one with the greatest upper bound of the two, so that the delta is non-zero. Hence we define $z_* \equiv \min(z_1, z_2)$. Note also that because of $\delta^3(\boldsymbol{k}+\boldsymbol{k}')$ we can continue our calculations considering $\boldsymbol{k} = -\boldsymbol{k}'$, which as A_k and z only depend on k through its square, the minus sign will be irrelevant. We proceed our calculation:

$$\begin{aligned}\langle \phi_k(z_1)\phi_{k'}(z_2)\rangle = -2H^{-3}(2\pi)^3\delta^3(\boldsymbol{k}+\boldsymbol{k}')z_1^{-\frac{1}{2}}z_2^{-\frac{1}{2}}\int_{z_i}^{z_*} ds\; s^{-2} \\ \times \exp\left[\frac{A_k}{2}(z_1-s)\right]\exp\left[\frac{A_k}{2}(z_2-s)\right]\sin(z_1-s)\sin(z_2-s) \\ \times \frac{\Gamma_\phi(s)T(s)}{a^3(s)}.\end{aligned} \tag{6.15}$$

The overall minus sign comes from the fact that $z_i > z\ , \forall z$[3].

To our purposes we are interested in the equal-times correlator, so we set $z_1 = z_2 = z$, and it yields:

$$\begin{aligned}\langle \phi_k(z)\phi_{k'}(z)\rangle = -2H^{-3}(2\pi)^3\delta^3(\boldsymbol{k}+\boldsymbol{k}')z^{-1} \\ \times \int_{z_i}^{z} ds\; s^{-2}\exp\left[A_k(z-s)\right]\sin^2(z-s)\frac{\Gamma_\phi(s)T(s)}{a^3(s)}\end{aligned} \tag{6.17}$$

Rewriting a, T and Γ_ϕ as a function of z:

$$\begin{aligned}a(z) &= z_i z^{-1} \\ T(z) &= T_i z z_i^{-1} \\ \Gamma_\phi(z) &= A_k H z,\end{aligned} \tag{6.18}$$

[3]If we have the dummy variable running backwards, then:

$$\int_{+\infty}^{-\infty} dx\;\delta(x)f(x-x_0) = -\int_{-\infty}^{+\infty} dx\;\delta(x)f(x-x_0) = -f(x_0). \tag{6.16}$$

the previous integral then simplifies to:

$$\langle\phi_k(z_1)\phi_{k'}(z_2)\rangle = -2A_kH^{-2}T_i(2\pi)^3\delta^3(\boldsymbol{k}+\boldsymbol{k}')z_i^{-4}z^{-1}\int_{z_i}^{z} ds\ s^3\exp\left[A_k(z-s)\right] \sin^2(z-s). \tag{6.19}$$

To avoid obtaining a too complicated integral, we saw above that the argument of the sine will be typically large and like so the sine will have an high frequency. So we can approximate it by its average $\langle\sin x\rangle = \frac{1}{2}$. We are then left with:

$$\langle\phi_k(z_1)\phi_{k'}(z_2)\rangle \simeq -A_kH^{-2}T_i(2\pi)^3\delta^3(\boldsymbol{k}+\boldsymbol{k}')z_i^{-4}z^{-1}\int_{z_i}^{z} ds\ s^3\exp\left[A_k(z-s)\right]. \tag{6.20}$$

The remaining integral yields:

$$\begin{aligned}\int_{z_i}^{z} ds\ s^3\exp\left[A_k(z-s)\right] &= -\exp[A_k(z-s)]\frac{6+6A_ks+3A_k^2s^2+A_k^3s^3}{A_k^4}\Bigg|_{z_i}^{z}, \\ &\simeq -\exp[A_k(z-s)]s^3A_k^{-1}\Big|_{z_i}^{z},\end{aligned} \tag{6.21}$$

where $A_kz \gg 1$ during thermal inflation.

Finally, the full variance of ϕ_k is:

$$\langle\phi_k(z_1)\phi_{k'}(z_2)\rangle \simeq (2\pi)^3\delta^3(\boldsymbol{k}+\boldsymbol{k}')\frac{T}{a^3\omega_k^2}\left[1-\exp\left(\frac{\Gamma_\phi(z)}{H}-\frac{\Gamma_\phi(z_i)}{H}\right)a^3\right]. \tag{6.22}$$

Shortly after the onset of thermal inflation the exponential term tends to zero as $\Gamma_\phi(z_i) \gg \Gamma_\phi(z) \gg H$ during thermal inflation:

$$\langle\phi_k(t)\phi_{k'}(t)\rangle \approx (2\pi)^3\delta^3(\boldsymbol{k}+\boldsymbol{k}')\frac{T(t)}{a^3(t)\omega_k^2(t)}. \tag{6.23}$$

Hence, the two-point correlation function reaches an equilibrium configuration, independent of its initial conditions. For this to happen the coupling α must satisfy:

$$\alpha \gg \left(\frac{\sqrt{mM_0}}{M_p}\right)^{\frac{1}{4}}. \tag{6.24}$$

For $m \sim 10^3$ GeV and $M_0 \sim M_p$ the lower bound on the coupling is $\alpha \gg 0.01$.

If we consider the Fourier expansion of the flaton field ϕ:

$$\phi(t,\boldsymbol{x}) = \int\frac{d^3k}{(2\pi)^3}\ \phi_k(t)\exp(i\boldsymbol{k}\cdot\boldsymbol{x}), \tag{6.25}$$

we can easily see that $\langle\phi\rangle$ vanishes in the equilibrium state, while the field variance is given by:

$$\begin{aligned}\langle\phi(\boldsymbol{x})\phi(\boldsymbol{y})\rangle &= \int \frac{d^3k}{(2\pi)^3}\frac{d^3k'}{(2\pi)^3}\ \langle\phi_k\phi_{k'}\rangle \exp(i\boldsymbol{k}\cdot\boldsymbol{x})\exp(i\boldsymbol{k}'\cdot\boldsymbol{y}) \\ &= \frac{T}{a^3}\int \frac{d^3k}{(2\pi)^3}\ \frac{1}{\omega_k^2}\exp[i\boldsymbol{k}\cdot(\boldsymbol{x}-\boldsymbol{y})],\end{aligned} \tag{6.26}$$

where we used equation (6.23) for the correlation of the field modes. If the fields are evaluated at the same point in space this becomes:

$$\langle\phi^2\rangle = \frac{1}{2\pi^2}\frac{T}{a}\int_0^{k_{\max}} dk\ \frac{k^2}{k^2+T_i^2\alpha^2} = \frac{2\alpha T^2}{(2\pi)^2}\left[\frac{k_{\max}}{\alpha T_i} - \arctan\left(\frac{k_{\max}}{\alpha T_i}\right)\right]. \tag{6.27}$$

Where we have defined $k_{\max}$ as the momentum cut-off needed for the field's variance to be finite. We will argue and try to motivate a physically appropriate cut-off shortly.

Bellow, we will need the correlation:

$$\langle\phi(0)\phi(\boldsymbol{x})\rangle^2 = \frac{T^2}{a^6}\int \frac{d^3k}{(2\pi)^3}\frac{d^3k'}{(2\pi)^3}\ \frac{1}{\omega_k^2}\frac{1}{\omega_{k'}^2}\exp[-i\boldsymbol{x}\cdot(\boldsymbol{k}+\boldsymbol{k}')], \tag{6.28}$$

so we leave it here for further reference.

Momentum cut-off

We now discuss the value of the momentum cut-off $k_{\max}$. During thermal inflation we have a radiation bath in equilibrium and a flaton field that begins out of equilibrium but, due to its interactions with the former, approaches equilibrium as we have shown. In the radiation bath, modes will be excited up to $p \sim T$ or in covariant momentum k, $k \sim T_i$, as higher modes will be Boltzmann suppressed. On the other hand we have referred in section 5.1.2 that the differential equation that we have solved for the flaton, equation (5.5), is only valid up to momenta $p \sim \pi T$, or $k \sim \pi T_i$ [34]. It is therefore sensible to consider $k_{max} = \pi T_i$. With this cut-off $\langle\phi^2\rangle$ becomes:

$$\langle\phi^2\rangle = \frac{1}{2\pi^2}\frac{T}{a}\int_0^{k_{\max}} dk\ \frac{k^2}{k^2+T_i^2\alpha^2} = \frac{2\alpha T^2}{(2\pi)^2}\left[\frac{\pi}{\alpha} - \arctan\left(\frac{\pi}{\alpha}\right)\right]. \tag{6.29}$$

6.2.2 The power spectrum

When calculating the power spectrum of the curvature perturbations we will be mainly interested in super-horizon modes $k \ll aH$, since these modes will remain

frozen until horizon re-entry later in the radiation era [3, 4]. The modes at horizon scale can be expressed as:

$$aH = \frac{T_i}{T} H \sim \alpha \frac{T_c}{T} \frac{M_0}{M_p} T_i, \tag{6.30}$$

which are always smaller then the cut-off momentum $k_{max} = \pi T_i$, given that the VEV M_0 is not Planckian.

Hence, we note that, while all thermalized modes contribute to the overall variance of the flaton field, the power spectrum will refer only to its long-wavelength fluctuations.

Consider now the variance of the field (6.27) computed above, alongside the variances of the field velocity (D.13) and gradient (D.16) computed in Appendix D. We restate them here as they appear in $\langle \rho \rangle$:

$$\begin{aligned} \frac{1}{2}\alpha^2 T^2 \langle \phi^2 \rangle &= \frac{\alpha^3 T^4}{(2\pi)^2} \left[\frac{\pi}{\alpha} - \arctan\left(\frac{\pi}{\alpha}\right) \right] \\ \frac{1}{2} \langle \dot{\phi}^2 \rangle &= \frac{\pi T^4}{12} \\ \frac{1}{2} a^{-2} \langle \partial_i \phi \partial_i \phi \rangle &= \frac{\pi T^4}{12} - \frac{\alpha^3 T^4}{(2\pi)^2} \left[\frac{\pi}{\alpha} - \arctan\left(\frac{\pi}{\alpha}\right) \right]. \end{aligned} \tag{6.31}$$

We see that all terms of $\langle \rho \rangle$ (6.9) that contribute to $\langle \dot{\rho} \rangle$ are proportional to T^4:

$$\langle \dot{\rho} \rangle = \frac{d}{dt} \left(\frac{\pi^2}{30} g_* T^4 + \frac{\pi T^4}{6} \right). \tag{6.32}$$

We may therefore account for the extra term as a bosonic degree of freedom, redefining g_*:

$$g_* = \frac{7}{8} n_f + \frac{5}{\pi}. \tag{6.33}$$

Thus the flaton yields an $\mathcal{O}(1)$ contribution to the number of relativistic degrees of freedom in the thermal bath, which explicitly shows that it has reached thermal equilibrium for $\Gamma_\phi \gtrsim H$, and further validates our choice for the (approximate) momentum cut-off.

Resuming the calculation of $\langle \dot{\rho} \rangle$:

$$\begin{aligned} \langle \dot{\rho} \rangle &= \frac{d}{dt} \left(\frac{\pi^2}{30} g_* T^4 \right), \\ &= -\frac{2\pi^2}{15} g_* T^4 H. \end{aligned} \tag{6.34}$$

Focusing now on the power spectrum $\mathcal{P}_\zeta$ (6.6), inserting (6.5) we obtain:

$$\begin{aligned}\mathcal{P}_\zeta &= \frac{k^3}{2\pi^2}\frac{H^2}{\langle\dot{\rho}\rangle^2}\int d^3x\ \exp(-i\boldsymbol{k}\cdot\boldsymbol{x})\,\langle\delta\rho(0)\delta\rho(\boldsymbol{x})\rangle\,,\\ &= \frac{225}{8\pi^6}\frac{k^3}{g_*^2T^8}\int d^3x\ \exp(-i\boldsymbol{k}\cdot\boldsymbol{x})\,\langle\delta\rho(0)\delta\rho(\boldsymbol{x})\rangle\,.\end{aligned} \tag{6.35}$$

By examining (6.10) we see that the total power spectrum will have contributions from all combinations of:

$$\langle\delta(X_i(0)^2)\delta(X_j(\boldsymbol{x})^2)\rangle = \langle\big(X_i^2(0)-\langle X_i^2\rangle\big)\big(X_j^2(\boldsymbol{x})-\langle X_j^2\rangle\big)\rangle \tag{6.36}$$

with differing prefactors. Where we take $X_1=\phi$, $X_2=\dot{\phi}$ and $X_3=\partial_i\phi$, which are all Gaussian variables.

As none of the $\langle X_i^2\rangle$ depends on space, we have that:

$$\langle\delta(X_i(0)^2)\delta(X_j(\boldsymbol{x})^2)\rangle = \langle X_i(0)^2X_j(\boldsymbol{x})^2\rangle - \langle X_i^2\rangle\langle X_j^2\rangle\,. \tag{6.37}$$

The first term on the right-hand side are 4th moments involving the Gaussian variables ϕ, $\dot{\phi}$ and $\partial_i\phi$. As it turns out there is a theorem due to Leon Isserlis [51] that allows for writing a kth moment of zero-average Gaussian variables in terms of their variance. For the 4th moment involving four zero-average Gaussian variables $\{X_1,X_2,X_3,X_4\}$ the theorem reads [52]:

$$\langle X_1X_2X_3X_4\rangle = \langle X_1X_2\rangle\langle X_3X_4\rangle + \langle X_1X_3\rangle\langle X_2X_4\rangle + \langle X_1X_4\rangle\langle X_2X_3\rangle\,. \tag{6.38}$$

For the case at hand we have:

$$\langle X_iX_iX_jX_j\rangle = \langle X_i^2\rangle\langle X_j^2\rangle + 2\langle X_iX_j\rangle^2\,. \tag{6.39}$$

This means that the generic perturbation (6.37) will simply be:

$$\langle\delta(X_i(0)^2)\delta(X_j(\boldsymbol{x})^2)\rangle = 2\langle X_i(0)X_j(\boldsymbol{x})\rangle^2\,. \tag{6.40}$$

The two-point correlation function for the energy density is then:

$$\begin{aligned}\langle\delta\rho(0)\delta\rho(\boldsymbol{x})\rangle = \frac{1}{2}\alpha^4T^4\langle\phi(0)\phi(\boldsymbol{x})\rangle^2 + \alpha^2T^2\langle\phi(0)\dot{\phi}(\boldsymbol{x})\rangle^2 + a^{-2}\alpha^2T^2\langle\phi(0)\partial_i\phi(\boldsymbol{x})\rangle^2\,,\\ + \frac{1}{2}\langle\dot{\phi}(0)\dot{\phi}(\boldsymbol{x})\rangle^2 + a^{-2}\langle\dot{\phi}(0)\partial_i\phi(\boldsymbol{x})\rangle^2 + \frac{1}{2}a^{-4}\langle\partial_i\phi(0)\partial_j\phi(\boldsymbol{x})\rangle^2\,,\end{aligned} \tag{6.41}$$

where we have used that thermal perturbations are classical and, hence, commute. This means that the power spectrum will have contributions from all possible correlations between ϕ, $\dot{\phi}$ and $\partial_i\phi$.

We will consider only the field–field term $\langle\phi(0)\phi(\boldsymbol{x})\rangle^2$ (6.28) for now, and discuss the others later. We have:

$$\int d^3x\ \exp(-i\boldsymbol{k}\cdot\boldsymbol{x})\frac{1}{2}\alpha^4T^4\left\langle\phi(0)\phi(\boldsymbol{x})\right\rangle^2 = \frac{1}{2}\alpha^4\frac{T^6}{a^6}\int\frac{d^3k_1}{(2\pi)^3}\frac{d^3k_2}{(2\pi)^3}\frac{1}{\omega_{k_1}^2}\frac{1}{\omega_{k_2}^2} \times\int d^3x\ \exp[-i\boldsymbol{x}\cdot(\boldsymbol{k}+\boldsymbol{k}_1+\boldsymbol{k}_2)], \tag{6.42}$$

The $\boldsymbol{x}$ integration is trivial:

$$\int d^3x\ \exp[-i\boldsymbol{x}\cdot(\boldsymbol{k}+\boldsymbol{k}_1+\boldsymbol{k}_2)] = (2\pi)^3\delta^3(\boldsymbol{k}+\boldsymbol{k}_1+\boldsymbol{k}_2), \tag{6.43}$$

effectively making $\boldsymbol{k}_2 = -\boldsymbol{k}-\boldsymbol{k}_1$ in the field–field contribution:

$$\begin{aligned}\int d^3\exp(-i\boldsymbol{k}\cdot\boldsymbol{x})\frac{1}{2}\alpha^4T^4\left\langle\phi(0)\phi(\boldsymbol{x})\right\rangle^2 &= \frac{1}{2}\alpha^4\frac{T^6}{a^6}\int\frac{d^3k_1}{(2\pi)^3}\frac{1}{\omega_{k_1}^2}\frac{1}{\omega_{k+k_1}^2}\\ &= \frac{1}{2}\alpha^4\frac{T^6}{a^2}\int\frac{d^3k_1}{(2\pi)^3}\frac{1}{k_1^2+\alpha^2T_i^2}\\ &\quad\times\frac{1}{(\boldsymbol{k}+\boldsymbol{k}_1)^2+\alpha^2T_i^2}.\end{aligned} \tag{6.44}$$

We first note that this contribution to the power spectrum does not diverge like the field variance (6.27) would. Nevertheless, we must still integrate up to $k_{\text{max}} = \pi T_i$, since our results are only valid up to that momentum.

We must keep in mind that we are just considering super-horizon modes with $k \ll T_i$ (cf. (6.30)), so that we may safely neglect k in the integral above:

$$\begin{aligned}\int\frac{d^3k_1}{(2\pi)^3}\frac{1}{k_1^2+\alpha^2T_i^2}\frac{1}{(\boldsymbol{k}+\boldsymbol{k}_1)^2+\alpha^2T_i^2} &\approx \frac{2}{(2\pi)^2}\int_0^{\pi T_i}dk_1\ \frac{k_1^2}{(k_1^2+\alpha^2T_i^2)^2},\\ &\approx \frac{1}{(2\pi)^2}\frac{1}{aT}\left[-\frac{\pi}{\alpha^2+\pi^2}+\alpha^{-1}\arctan\left(\pi\alpha^{-1}\right)\right].\end{aligned} \tag{6.45}$$

The field–field contribution to the power-spectrum is then:

$$\int d^3\exp(-i\boldsymbol{k}\cdot\boldsymbol{x})\frac{1}{2}\alpha^4T^4\left\langle\phi(0)\phi(\boldsymbol{x})\right\rangle^2 = \frac{\alpha^3}{(2\pi)^2}\frac{T^5}{a^3}\left[-\frac{1}{2}\frac{\pi\alpha}{\alpha^2+\pi^2}+\frac{1}{2}\arctan\left(\pi\alpha^{-1}\right)\right]. \tag{6.46}$$

Before presenting the full power spectrum we must check how the other terms in equation (6.41) affect the overall result. The calculations are similar to the one above

so we leave the details in appendix E and simply state those results here:

$$\begin{aligned}
\int d^3x\ \exp(-i\boldsymbol{k}\cdot\boldsymbol{x})\alpha^2T^2\left\langle\phi(0)\dot{\phi}(\boldsymbol{x})\right\rangle^2 &= \frac{1}{2}\left(\frac{3\alpha^3}{16\pi}\right)^2 \\
&\quad\times\int d^3x\ \exp(-i\boldsymbol{k}\cdot\boldsymbol{x})\frac{1}{2}\alpha^4T^4\left\langle\phi(0)\phi(\boldsymbol{x})\right\rangle^2, \\
\int d^3x\ \exp(-i\boldsymbol{k}\cdot\boldsymbol{x})\frac{1}{2}\left\langle\dot{\phi}(0)\dot{\phi}(\boldsymbol{x})\right\rangle^2 &= \frac{\pi}{12}\frac{T^5}{a^3}, \\
\int d^3x\ \exp(-i\boldsymbol{k}\cdot\boldsymbol{x})a^{-2}\alpha^2T^2\left\langle\phi(0)\partial_i\phi(\boldsymbol{x})\right\rangle^2 &\approx \frac{\alpha^3}{(2\pi)^2}\frac{T^5}{a^3} \\
&\quad\times\left[\frac{2\pi}{\alpha}+\frac{\alpha\pi}{\left(\alpha^2+\pi^2\right)}-3\arctan\left(\pi\alpha^{-1}\right)\right], \qquad (6.47) \\
\int d^3x\ \exp(-i\boldsymbol{k}\cdot\boldsymbol{x})a^{-2}\left\langle\dot{\phi}(0)\partial_i\phi(\boldsymbol{x})\right\rangle^2 &= \left(\frac{3\alpha^3}{32\pi}\right)^2 \\
&\quad\times\int d^3x\ \exp(-i\boldsymbol{k}\cdot\boldsymbol{x})a^{-2}\alpha^2T^2\left\langle\phi(0)\partial_i\phi(\boldsymbol{x})\right\rangle^2, \\
\int d^3x\ \exp(-i\boldsymbol{k}\cdot\boldsymbol{x})\frac{1}{2}a^{-4}\left\langle\partial_i\phi(0)\partial_i\phi(\boldsymbol{x})\right\rangle^2 &\approx \frac{\alpha^3}{(2\pi)^2}\frac{T^5}{a^3} \\
&\quad\times\left[-2\frac{\pi}{\alpha}+\frac{\pi^3}{3\alpha^3}-\frac{\alpha\pi}{2(\alpha^2+\pi^2)}+\frac{5}{2}\arctan\left(\pi\alpha^{-1}\right)\right].
\end{aligned}$$

By inspecting these terms we see that they all have the same dependence on the ratio $\frac{T^5}{a^3}$ as the field-field contribution (6.46). This is another consequence of field having reached equilibrium with the ambient thermal bath. We notice, however, that the field–kinetic and the kinetic–gradient contributions can be neglected compared to the field–field and the field–gradient contributions, respectively.

With all contributions accounted for, we now write the full the power spectrum $\mathcal{P}_\zeta^{(\text{therm})}$ valid for super-horizon modes:

$$\mathcal{P}_\zeta^{(\text{therm})}(k) = \frac{150}{(2\pi)^5}\frac{k^3}{g_*^2T_i^3}, \qquad (6.48)$$

the superscript (therm) will label the thermal power spectrum computed in this thesis to distinguish it from the quantum one computed in [10].

We see that the power spectrum is blue-tilted, increasing with k^3. Therefore, the largest perturbations will correspond to the last scales to become super-horizon during thermal inflation, i.e. close to the critical temperature:

$$k_c = a_cH = \alpha T_i\frac{H}{m}, \qquad (6.49)$$

where a_c is the scale factor at the critical temperature. Thus, we obtain the maximum value of the power spectrum produced during thermal inflation:

$$\mathcal{P}_\zeta^{(\text{therm, max})}(k_c) = \frac{150}{(2\pi)^5}\frac{\alpha^3}{g_*^2}\left(\frac{H}{m}\right)^3. \tag{6.50}$$

This expression depends on the flaton's coupling to the thermal bath α, the number of relativistic degrees of freedom g_* and the ratio $\frac{H}{m}$ which can be rewritten in terms of the flaton's VEV M_0:

$$\frac{H}{m} \approx \frac{M_0}{3M_p}. \tag{6.51}$$

We thus conclude that the power spectrum will be suppressed if the flaton's VEV is kept sub-Planckian. We get an additional suppression due to the fermions in the thermal bath, $g_* \approx 100$, as we are dealing with temperatures surely above the rest mass of all standard model particles.

Now we compare our maximum with the one computed in [10, eq (2.24)] which only took into account the quantum fluctuations of the flaton field, discarding any thermal fluctuation-dissipation effects. Temperature considerations were only attended to describe the thermal mass, which is fundamental for the existence of a phase transition near the critical temperature. The authors found[4]:

$$\begin{aligned}\mathcal{P}_\zeta^{(\text{quan, max})}(k_{\text{peak}}) \approx & \frac{12m_{\text{eff}}^4\left(\frac{a^2H^2}{m^2}\right)^\nu {}_2F_1\left(\frac{3}{2},\nu;\frac{5}{2},-\frac{a^2H^2}{m^2}\right)}{\left\{\partial_{N_e}\left[m_{\text{eff}}^2\left(\frac{a^2H^2}{m^2}\right)^\nu {}_2F_1\left(\frac{3}{2},\nu;\frac{5}{2},-\frac{a^2H^2}{m^2}\right)\right]\right\}^2}, \\ & \left(\frac{\sqrt{3(2\nu+3)}}{2a}\right)^3\left[\frac{3(2\nu+3)}{4a^2}+\frac{m^2}{a^2H^2}\right]^{-\nu},\end{aligned} \tag{6.52}$$

where $\nu = \sqrt{\frac{9}{4}+\frac{m^2}{H^2}}$ and k_{peak} is the momentum that maximizes the quantum power spectrum (denoted k_{max} in [10]). The authors set the scale factor to one at the critical temperature, $a(T_c) = 1$, so their effective mass differs from our definition:

$$m_{\text{eff}}^{(\text{quan})} = m\sqrt{-1+a^{-2}}. \tag{6.53}$$

It is important to bear in mind that, on the one hand, equation (6.52) evaluated at k_{peak} describes how the maximum of $\mathcal{P}_\zeta$ evolves with the number of e-folds, freezing out when k_{peak} exits the horizon. On the other hand, our equation (6.50) is the maximum value that $\mathcal{P}_\zeta$ could ever attain at super-horizon scales. We can see that both $\mathcal{P}_\zeta^{(\text{quan, max})}$ (6.52) and our expression $\mathcal{P}_\zeta^{(\text{therm, max})}$ (6.50) depend on the ratio $\frac{H}{m}$ but our result also depends on α and g_*. The quantum power spectrum from [10] does not

[4]Note that equation (6.52) is a root mean square approximation.

depend on α because the authors only considered thermal corrections to the flaton potential but not the full fluctuation-dissipation dynamics that lead to thermalization. Additionally the authors have neglected the contribution of the radiation bath ρ_{rad} to the total energy density, which explains why their result also does not depend on it through g_*.

We now compare the maximum of the power spectrum computed in this thesis $\mathcal{P}_\zeta^{(\text{therm, max})}$ (6.50) and the one from [10] (6.52), $\mathcal{P}_\zeta^{(\text{quan, max})}$, as a function of $\frac{H}{m}$, considering a strong coupling (figure 6.1). Both plots of $\mathcal{P}_\zeta^{\text{max}}$ have the same overall behavior, nevertheless, the thermal result is shifted to lower values, yielding a power-spectrum roughly 10^{-6} less intense than its quantum counterpart. The fact that the more apparent difference between them appears to be just a shift, might hint us that the difference is just a multiplicative factor. In fact, the authors in [10] have neglected the radiation bath contribution to $\langle\dot{\rho}\rangle$ and also, only considered super-horizon modes when calculating the variance of the field. This would result in their $\langle\dot{\rho}\rangle$ being larger than the one computed in this thesis, effectively driving the magnitude of their power spectrum up.

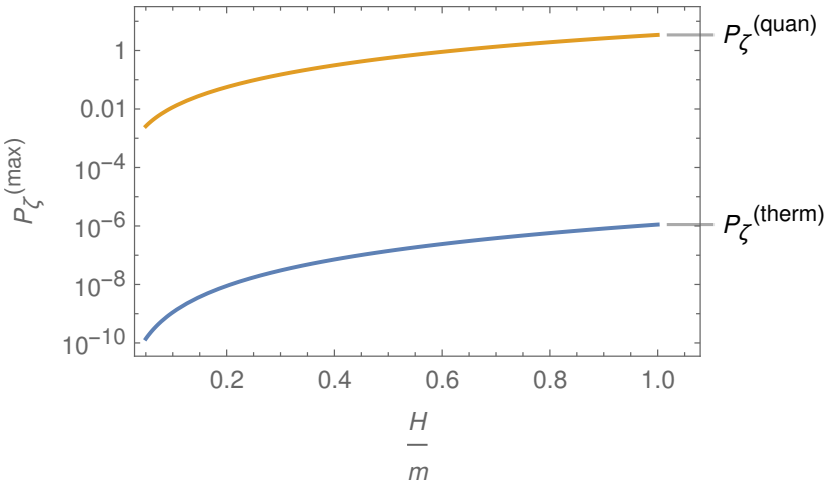

Figure 6.1: Plot of the maximum value of the thermal power spectrum (6.50) ($\mathcal{P}_\zeta^{(\text{therm})}$) and the quantum power spectrum (6.52) ($\mathcal{P}_\zeta^{(\text{quan})}$) as a function of of $\frac{H}{m}$. For the thermal plot we considered strong couplings $\alpha = 0.9$ and used $g_* = 100$.

The value of $\mathcal{P}_\zeta^{(\text{therm, max})}$ is greatly suppressed by g_* , which means that if the radiation bath were composed of fewer fermions the power spectrum would have a larger amplitude (figure 6.2).

Finally we note, that the larger the coupling α the greatest the peak of the curvature's power spectrum (Figure 6.3). This is solely a consequence of the maximum of the power spectrum occurring close to the critical point, according to equations (6.48) through (6.50).

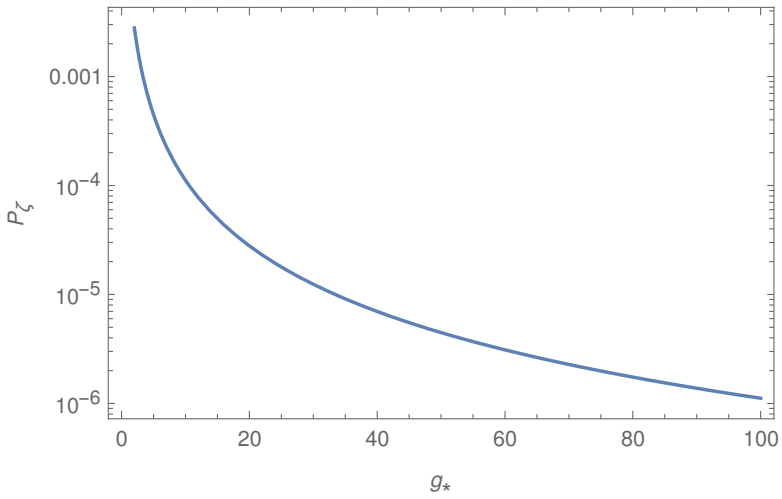

Figure 6.2: Plot of the maximum value of the thermal curvature power spectrum (6.50) as a function of the relativistic degrees of freedom g_*. To plot this graph we considered strong couplings $\alpha = 0.9$ and used $\frac{H}{m} = 1$.

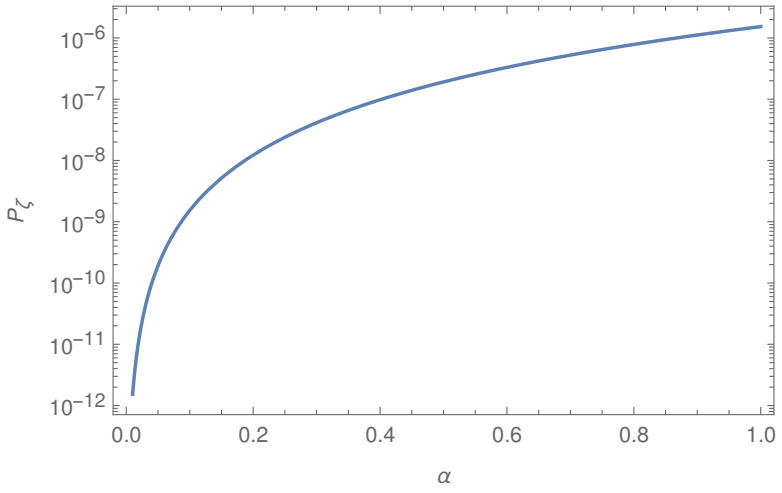

Figure 6.3: Plot of the power spectrum $\mathcal{P}_\zeta$, (6.50) as a function of the coupling α . To plot this graph we used $g_* = 100$ and $\frac{H}{m} = 1$.

Chapter 7

Discussion and conclusions

In this thesis, we have studied the dynamics of thermal inflation driven by a flaton scalar field, which is held in a false vacuum at the origin due to its interactions with the ambient radiation bath. We have, for the first time, computed the spectrum of curvature perturbations induced on super-horizon scales by thermal fluctuations of the flaton field. Our analysis was based on the Langevin-like equation satisfied by the flaton as a result of Yukawa interactions with fermions in the cosmic thermal bath, in accordance with the fluctuation-dissipation theorem.

At zero-temperature, the flaton's potential resulting from supersymmetry breaking and Planck-suppressed non-renormalizable terms has a non-trivial minimum. However, interactions with the ambient thermal bath generically induce a thermal mass that shifts the minimum to the origin at high temperatures. Due to the non-zero value of its potential energy at the origin, the flaton may act as an effective cosmological constant and drive a short period of inflation, presumed to occur after the main inflation period in the early universe. Such a thermal inflation period ends when the temperature of the thermal bath, which decreases exponentially fast, falls below a critical value and the field eventually settles into the true vacuum with vanishing potential energy. This short inflation period can help diluting any dangerous relics produced during the first reheating period after inflation, such as gravitinos (the graviton's superpartners) and moduli fields, showing how the inflationary paradigm can be used to reconcile supersymmetry/supergravity theories and similar scenarios with standard cosmology.

A recent article [10] claimed that perturbations in the flaton field could induce large curvature perturbations during thermal inflation. These are small-scale perturbations, given that scales leaving the horizon during this period are much smaller than those that became super-horizon during the first inflationary epoch. This would later result in large overdensities in the universe during the radiation era that could promptly collapse into black holes upon horizon re-entry. Such a copious production of primordial black holes could be enticing and have a very significant cosmological impact, since they could account for at least a fraction of dark matter. Nevertheless, this study did

not take into account the fluctuation-dissipation effects induced by the thermal bath on the dynamics of flaton perturbations, which motivated the analysis performed in this thesis.

Our work revealed that the power spectrum of curvature perturbations in the regime where the flaton thermalizes with the ambient radiation bath is much more suppressed, by a factor $\sim 10^{-6}$ for $g_* \sim 100$, than the one computed in [10] assuming a purely quantum nature for flaton fluctuations. This is due not only to the larger variance of the flaton field in the thermalized case but also to the inclusion, in our analysis, of the overall contribution of the radiation bath to the total energy density, which was discarded in [10].

It is fruitful to review the assumptions that we have made throughout this work. We assumed that the flaton started close to the origin at the onset of thermal inflation, which is justified since the field is quickly driven to the minimum of the potential by Hubble expansion and thermal decay. We did not impose, however, that the field was already in thermal equilibrium with the radiation bath but rather showed that this would necessarily happen during thermal inflation provided that the effective coupling α of the flaton to the fields in the thermal bath is not too suppressed, i.e $\alpha \gg 0.01$ (cf. (6.24)). So that a strong coupling ($\alpha \sim 1$) was also an assumption in this thesis.

In our analysis of the Langevin-like equation for flaton modes we made two approximations that allowed for obtaining simple analytical solutions: (1) the thermal mass dominates over the zero-temperature contribution; and (2) the flaton's thermal decay width is larger than the Hubble expansion rate. We showed that such approximations are sufficiently good throughout thermal inflation up to close to the phase transition, again provided that the flaton's coupling to the thermal bath is sufficiently strong.

A possible source of theoretical error in our analysis is the momentum cut-off which is necessary to compute the variance of the flaton field, and hence its contribution to the average energy density. Such a cut-off would not be necessary had we used a more exact expression for the noise correlation function, rather than a Gaussian white noise approximation. Nevertheless, our choice for the cut-off value at the temperature of the thermal bath is physically sensible and supported by previous analyses [34], and up to $\mathcal{O}(1)$ factors it should yield the correct magnitude and parametric form for the power spectrum.

Our results show that the curvature perturbations produced during thermal inflation are too small to promptly collapse into primordial black holes upon horizon reentry. Of course the power spectrum gives the variance of a Gaussian distribution for curvature perturbations, and there will always be a small fraction of large overdensities at the tail of the distribution that could generate such black holes, but our analysis suggests that this is exponentially suppressed and therefore negligible in terms of, in particular, accounting for any sizable fraction of dark matter.

In the purely quantum case considered in [10] the variance of the field is restricted to super-horizon modes and therefore much smaller than in the thermal case that we have studied in this thesis. Alongside neglecting the radiation's contribution to the total energy density, this justifies the much larger value for the curvature's power spectrum $\mathcal{P}_\zeta$ (see equation (2.16) found in [10]). As a matter of fact, even if there were any argument that could change the momentum cut-off which resulted in obtaining smaller contributions from the variances of the field and its derivative, the contribution from the thermal bath would still drive down the magnitude of the power spectrum.

We should nevertheless mention that, strictly speaking, our analysis is not valid very close to the critical temperature at which the phase transition occurs, since at this stage we cannot fully neglect the zero-temperature contribution to the effective mass of the flaton. As argued in [10], this is when the concavity of the potential changes and larger curvature fluctuations could arise, as is a common critical behavior of many physical systems. We would therefore like to extend our analysis to this regime in the future. Moreover, a period of fast roll inflation [53] may follow the phase transition in some scenarios, which may have consequences for the amplitude of the power spectrum, also to be examined in future work.

All these aspects may come to change our preliminary conclusion that thermal inflation cannot lead to a significant population of primordial black holes. We note, however, that our results yield, nevertheless, a larger power spectrum on small scales than what is inferred from CMB measurements on large scales, i.e. $\mathcal{P}_\zeta \sim 10^{-9}$. This could naturally have consequences for cosmological structure formation, such that the present thesis also motivates further research in this topic.

Appendix A

Curvature in general relativity

Here we will gather some information concerning manifolds that will be useful in the main text. This will be mainly related to the curvature of a manifold, which is an essential tool of general relativity. For a more complete understanding see for example [22, 23].

For a space-time with a general metric $g_{\mu\nu}$ the partial derivative ∂_μ will not be a proper one-form. So we must define the covariant derivative ∇_μ. Acting on a vector it reads:

$$\nabla_\mu V^\nu = \partial_\mu V^\nu + \Gamma^\nu_{\mu\lambda} V^\lambda, \tag{A.1}$$

where $\Gamma^\nu_{\mu\sigma}$ are the Christoffel symbols which are related to the metric by:

$$\Gamma^\nu_{\mu\sigma} = \frac{1}{2} g^{\nu\lambda}(\partial_\mu g_{\sigma\lambda} + \partial_\sigma g_{\lambda\mu} - \partial_\lambda g_{\mu\sigma}). \tag{A.2}$$

The covariant derivative acting on one-form is:

$$\nabla_\mu \omega_\nu = \partial_\mu \omega_\nu - \Gamma^\lambda_{\mu\nu} \omega_\lambda, \tag{A.3}$$

while the covariant derivative of a $(0,2)$ tensor A is given by:

$$\nabla_\mu A^{\sigma\nu} = \partial_\mu A^{\sigma\nu} + \Gamma^\sigma_{\mu\lambda} A^{\lambda\nu} + \Gamma^\nu_{\mu\lambda} A^{\sigma\lambda}. \tag{A.4}$$

The curvature of a space-time is described by the Riemann tensor $R^\rho{}_{\sigma\mu\nu}$, which is given by:

$$R^\rho{}_{\sigma\mu\nu} = \partial_\mu \Gamma^\rho_{\nu\sigma} - \partial_\nu \Gamma^\rho_{\mu\sigma} + \Gamma^\rho_{\mu\lambda}\Gamma^\lambda_{\nu\sigma} - \Gamma^\rho_{\nu\lambda}\Gamma^\lambda_{\mu\sigma}. \tag{A.5}$$

From the Riemann tensor we obtain the Ricci tensor $R_{\mu\nu}$, contracting the the first and third indices of the former:

$$R_{\mu\nu} = R^\lambda{}_{\mu\lambda\nu}, \tag{A.6}$$

and the Ricci scalar R is obtained by contracting the Ricci tensor into a scalar:

$$R = R^\mu{}_\mu. \tag{A.7}$$

This two tensors can be combined to yield the Einstein tensor $G_{\mu\nu}$:

$$G_{\mu\nu} = R_{\mu\nu} - \frac{1}{2} R g_{\mu\nu}. \tag{A.8}$$

Appendix B

Robertson-Walker geometry

This appendix is devoted to the geometry of the Robertson-Walker manifold using spherical coordinates for the spatial part, (t, r, θ, ϕ), labeled $(0, 1, 2, 3)$, respectively. We will list here the Christoffel symbols $\Gamma^{\lambda}_{\mu\nu}$ needed to take covariant derivatives and the Ricci tensor $R_{\mu\nu}$, the Ricci scalar R and Einstein tensor $G_{\mu\nu}$ that are required to obtain Einstein's equation. For completeness we present the Robertson-Walker metric:

$$ds^2 = -dt^2 + a^2(t)\left(\frac{dr^2}{1-\kappa r^2} + r^2 d\theta^2 + r^2 \sin^2\theta d\phi^2\right). \tag{B.1}$$

We write the non-zero Christoffel symbols $\Gamma^{\lambda}_{\mu\nu}$ which is symmetric in its lower indices:

$$\begin{aligned}
\Gamma^0_{ij} &= H g_{ij} \\
\Gamma^1_{11} &= \frac{\kappa r}{1-\kappa r^2} \\
\Gamma^1_{01} &= \Gamma^2_{02} = \Gamma^3_{03} = H \\
\Gamma^1_{22} &= -r(1-\kappa r^2) \\
\Gamma^1_{33} &= -r\sin^2\theta(1-\kappa r^2) \\
\Gamma^2_{12} &= \Gamma^3_{13} = \frac{1}{r} \\
\Gamma^2_{33} &= -\sin\theta\cos\theta \\
\Gamma^3_{32} &= \cot\theta.
\end{aligned} \tag{B.2}$$

Next we have the non-zero components of the Ricci tensor:

$$\begin{aligned}
R_{00} &= -3\frac{\ddot{a}}{a} \\
R_{ij} &= \left(\frac{\ddot{a}}{a} + \frac{2\dot{a}^2}{a^2} + \frac{2\kappa}{a^2}\right) g_{ij},
\end{aligned} \tag{B.3}$$

and by contracting the Ricci tensor, we obtain the Ricci scalar:

$$R = g^{\mu\nu} R_{\mu\nu} = 6\left(\frac{\ddot{a}}{a} + \frac{\dot{a}^2}{a^2} + \frac{\kappa}{a^2}\right). \tag{B.4}$$

Finally, the Einstein tensor is given by:

$$\begin{aligned} G_{00} &= 3\left(\frac{\dot{a}^2}{a^2} + \frac{\kappa}{a^2}\right) \\ G_{ij} &= -\left(\frac{2\ddot{a}}{a} + \frac{\dot{a}^2}{a^2} + \frac{\kappa}{a^2}\right) g_{ij}. \end{aligned} \tag{B.5}$$

Appendix C

Fluctuation-dissipation relation in terms of the z variable

In section 5.2 we defined the dimensionless variable z (5.15), which we restate here:

$$z = z_i \exp(-Ht), \tag{C.1}$$

with $z_i = H^{-1}\sqrt{k^2 + \alpha^2 T_i^2}$. We would like to translate the fluctuation-dissipation relation (5.6) from time t to z, so that we may call upon it when convenient. Starting with the said relation:

$$\langle \xi_k(t_1)\xi_{k'}(t_2)\rangle = 2\Gamma_\phi(k)T\frac{(2\pi)^3}{a^3}\delta^3(\boldsymbol{k}+\boldsymbol{k'})\delta(t_1 - t_2). \tag{C.2}$$

Time can be written as a function of z by inverting (C.1):

$$t(z) = H^{-1}\ln\left(\frac{z_i}{z}\right), \tag{C.3}$$

so we can consider the argument of the delta function as a function of z:

$$\langle \xi_k(t_1(z_1))\xi_{k'}(t_2)\rangle = 2\Gamma_\phi(z_1)T(z_1)\frac{(2\pi)^3}{a^3(z_1)}\delta^3(\boldsymbol{k}+\boldsymbol{k'})\delta(t_1(z_1) - t_2(z_2)). \tag{C.4}$$

Using the general result [46]:

$$\delta(g(x)) = \sum_i \frac{\delta(x - x_i)}{|g'(x_i)|} \tag{C.5}$$

where x_i is the i-th root of the function $g(x)$. We see that we have a single root for $z_1 = z_2$ which means that (C.2) in terms of the dimensionless z is given by:

$$\langle \xi_k(z_1)\xi_{k'}(z_2)\rangle = 2Hz_1\Gamma_\phi(z_1)T(z_1)\frac{(2\pi)^3}{a^3(z_1)}\delta^3(\boldsymbol{k}+\boldsymbol{k'})\delta(z_1 - z_2). \tag{C.6}$$

Appendix D

Variances and correlations

In this section we compute the variances $\langle \dot{\phi}^2 \rangle$ and $\langle \partial\phi\partial_i\phi \rangle$ that contribute to $\langle \dot{\rho} \rangle$. We also present correlations between the relevant field and field derivatives that partake in the calculation of the power spectrum $\mathcal{P}_\zeta$.

It is good to keep in mind that all of these quantities ultimately stem from the particular solution $\phi_k^{(p)}$ (5.43):

$$\phi_k^{(p)}(z) = H^{-2} \int_{z_i}^{z} ds\, s^{-2} G_s(z,s) \xi_k(s), \tag{D.1}$$

with:

$$G_s(z,s) = \left(\frac{s}{z}\right)^{\frac{1}{2}} \exp\left[\frac{A_k}{2}(z-s)\right] \sin(z-s). \tag{D.2}$$

D.1 Field velocity variance

Differentiating the particular solution (D.1) we get:

$$\begin{aligned} \dot{\phi}_k^{(p)} &= -H^{-1} z \int_{z_i}^{z} ds\, s^{-2} \xi_k(s) \partial_z G_s(z,s) \\ &= -H^{-1} z^{\frac{1}{2}} \int_{z_i}^{z} ds\, s^{-\frac{3}{2}} \exp\left[\frac{A_k}{2}(z-s)\right] \cos(z-s)\xi_k(s) + \frac{H}{2}(1 - A_k z)\phi_k{}^{(p)}. \end{aligned} \tag{D.3}$$

Where we have used the Leibniz integral rule and the fact that the Green's function has the property that $G_s(z,z) = 0$.

From this we can see that:

$$\langle \dot{\phi}_k \rangle = A\dot{m}_k + B\dot{u}_k, \tag{D.4}$$

consequently the decay of the flaton an Hubble expansion will make the field's velocity approach zero. In fact, both the homogeneous solutions (5.38) bear a decaying exponential meaning that their time derivative will also decay. So we have:

$$\langle \dot{\phi}_k \rangle = 0. \tag{D.5}$$

The variance is not such a trivial matter, it has the form:

$$\begin{aligned}
\langle \dot{\phi}_k(z_1)\dot{\phi}_{k'}(z_2)\rangle = H^{-2} z_1^{\frac{1}{2}} z_2^{\frac{1}{2}} \int_{z_i}^{z_1} ds_1 \int_{z_i}^{z_2} ds_2 \; s_1^{-\frac{3}{2}} s_2^{-\frac{3}{2}} \\
\times \exp\left[\frac{A_k}{2}(z_1 - s_1)\right] \exp\left[\frac{A_{k'}}{2}(z_2 - s_2)\right] \\
\times \cos(z_1 - s_1)\cos(z_2 - s_2)\,\langle \xi_k(s_1)\xi_{k'}(s_2)\rangle \\
+ \frac{H^2}{4}(1 - A_k z_1)(1 - A_{k'} z_2)\,\langle \phi_k(z_1)\phi_{k'}(z_2)\rangle \\
- \frac{H^{-2}}{2} z_1^{\frac{1}{2}}(1 - A_{k'} z_2) z_2^{-\frac{1}{2}} \int_{z_i}^{z_1} ds_1 \int_{z_i}^{z_2} ds_2 \; s_1^{-\frac{3}{2}} s_2^{-\frac{3}{2}} \\
\times \exp\left[\frac{A_k}{2}(z_1 - s_1)\right] \exp\left[\frac{A_{k'}}{2}(z_2 - s_2)\right] \\
\times \cos(z_1 - s_1)\sin(z_2 - s_2)\,\langle \xi_k(s_1)\xi_{k'}(s_2)\rangle \\
- \frac{H^{-2}}{2} z_2^{\frac{1}{2}}(1 - A_k z_1) z_1^{-\frac{1}{2}} \int_{z_i}^{z_1} ds_1 \int_{z_i}^{z_2} ds_2 \; s_1^{-\frac{3}{2}} s_2^{-\frac{3}{2}} \\
\times \exp\left[\frac{A_k}{2}(z_1 - s_1)\right] \exp\left[\frac{A_{k'}}{2}(z_2 - s_2)\right] \\
\times \cos(z_2 - s_2)\sin(z_1 - s_1)\,\langle \xi_k(s_1)\xi_{k'}(s_2)\rangle\,.
\end{aligned} \tag{D.6}$$

The intervening integrals are similar to the one in (6.13), solved in Section 6.2.1:

$$\begin{aligned}
\langle \phi_k(z_1)\phi_{k'}(z_2)\rangle = H^{-4} z_1^{-\frac{1}{2}} z_2^{-\frac{1}{2}} \int_{z_i}^{z_1} ds_1 \int_{z_i}^{z_2} ds_2 \; s_1^{-\frac{3}{2}} s_2^{-\frac{3}{2}} \\
\times \exp\left[\frac{A_k}{2}(z_1 - s_1)\right] \exp\left[\frac{A_{k'}}{2}(z_2 - s_2)\right] \\
\times \mathrm{trig}(z_1, z_2, s_1, s_2)\,\langle \xi_k(s_1)\xi_{k'}(s_2)\rangle\,.
\end{aligned} \tag{D.7}$$

Besides some prefactors the difference is where there was $\sin(z_1 - s_1)\sin(z_2 - s_2)$, in the present integrals are other combinations of sines and cosines, here denoted as «trig». In the section mentioned above the trig function was eventually averaged over, since it has an high frequency. Analogously, we may use:

$$\begin{aligned}
\langle \cos^2(x)\rangle &= \frac{1}{2} \\
\langle \cos(x)\sin(x)\rangle &= 0.
\end{aligned} \tag{D.8}$$

Setting first $z_1 = z_2 = z$, we see that the first integral is equal to $H^2 z^2 \langle \phi_k \phi_{k'} \rangle$ while the last two are zero. This of course is only approximately true. Nevertheless, $\langle \dot{\phi}_k \dot{\phi}_{k'} \rangle$ simplifies to:

$$\begin{aligned} \langle \dot{\phi}_k \dot{\phi}_{k'} \rangle \approx & H^2 \left[z^2 + \frac{1}{4}(1 - A_k z)^2 \right] \langle \phi_k \phi_{k'} \rangle \\ \approx & H^2 z^2 \left(1 + \frac{1}{4} A_k^2 \right) \\ \approx & H^2 z^2 \langle \phi_k \phi_k \rangle = \omega_k^2 \langle \phi_k \phi_k \rangle . \end{aligned} \tag{D.9}$$

Where we considered only the largest power of $z A_k$ due to its large value in the second line and used the smallness of A_k in the third line.

Applying the equilibrium form of the variance of the field modes (6.23), we get:

$$\langle \dot{\phi}_k \dot{\phi}_{k'} \rangle \approx (2\pi)^3 \delta^3(\boldsymbol{k} + \boldsymbol{k}') \frac{T}{a^3}, \tag{D.10}$$

which is mode independent.

The field's velocity $\dot{\phi}$ inherits from its modes a zero average:

$$\langle \dot{\phi} \rangle = 0. \tag{D.11}$$

In its turn, the variance of the field velocity in term of its Fourier modes is given by:

$$\begin{aligned} \langle \dot{\phi}(\boldsymbol{x}) \dot{\phi}(\boldsymbol{y}) \rangle &= \int \frac{d^3k}{(2\pi)^3} \frac{d^3k'}{(2\pi)^3} \ \langle \dot{\phi}_k \dot{\phi}_{k'} \rangle \exp(i\boldsymbol{k} \cdot \boldsymbol{x}) \exp(i\boldsymbol{k}' \cdot \boldsymbol{y}) \\ &= \frac{T}{a^3} \int \frac{d^3k}{(2\pi)^3} \ \exp[i\boldsymbol{k} \cdot (\boldsymbol{x} - \boldsymbol{y})]. \end{aligned} \tag{D.12}$$

Where we applied (D.9). If the fields are evaluated at the same point in space we have:

$$\langle \dot{\phi}^2 \rangle = \frac{2}{(2\pi)^2} \frac{T}{a^3} \int_0^{k_{\max}} dk \ k^2 = \frac{2}{3(2\pi)^2} T^4 \frac{k_{\max}^3}{T_i^3}. \tag{D.13}$$

In the main text we will need the quantity:

$$\langle \dot{\phi}(0) \dot{\phi}(\boldsymbol{x}) \rangle^2 = \frac{T^2}{a^6} \int \frac{d^3k}{(2\pi)^3} \frac{d^3k'}{(2\pi)^3} \ \exp[-i\boldsymbol{x} \cdot (\boldsymbol{k} + \boldsymbol{k}')], \tag{D.14}$$

so we leave it here for further reference.

D.2 Field gradient variance

The variance of the field gradient in terms of ϕ_k is given by:

$$\begin{aligned}\langle \partial_i\phi(\boldsymbol{x})\partial_j\phi(\boldsymbol{y})\rangle &= -\int \frac{d^3k}{(2\pi)^3}\frac{d^3k'}{(2\pi)^3}\, k_i k'_j \,\langle \phi_k\phi_{k'}\rangle \exp(i\boldsymbol{k}\cdot\boldsymbol{x})\exp(i\boldsymbol{k}'\cdot\boldsymbol{y}) \\ &= \frac{T}{a^3}\int \frac{d^3k}{(2\pi)^3}\,\frac{k_ik_j}{\omega_k^2}\exp[i\boldsymbol{k}\cdot(\boldsymbol{x}-\boldsymbol{y})].\end{aligned} \tag{D.15}$$

Where we used equation (6.23) for the field variance. If the gradients are evaluated at the same spatial point then we get:

$$\begin{aligned}\langle \partial_i\phi\partial_i\phi\rangle &= \frac{2}{(2\pi)^2}\frac{T}{a}\int_0^{k_{\rm max}} dk\,\frac{k^4}{k^2+T_i^2\alpha^2} \\ &= \frac{1}{6\pi^2}\frac{T}{a}k_{\rm max}^3 - (\alpha T_i)^2\frac{\alpha T^2}{2\pi^2}\left[\frac{k_{\rm max}}{\alpha T_i} - \arctan\left(\frac{k_{\rm max}}{\alpha T_i}\right)\right] \\ &= 2a^2\Bigg\{-\alpha^3\frac{T^4}{(2\pi)^2}\left[\frac{k_{\rm max}}{\alpha T_i} - \arctan\left(\frac{k_{\rm max}}{\alpha T_i}\right)\right] + \frac{T^4}{3(2\pi)^2}\frac{k_{\rm max}^3}{T_i^3}\Bigg\}.\end{aligned} \tag{D.16}$$

Elsewhere we will also need the correlation:

$$\langle \partial_i\phi(0)\partial_j\phi(\boldsymbol{x})\rangle^2 = \frac{T^2}{a^6}\int \frac{d^3k}{(2\pi)^3}\frac{d^3k'}{(2\pi)^3}\,\frac{(\boldsymbol{k}\cdot\boldsymbol{k}')^2}{\omega_k^2\omega_{k'}^2}\exp[-i\boldsymbol{x}\cdot(\boldsymbol{k}+\boldsymbol{k}')], \tag{D.17}$$

so we leave it here for further reference.

D.3 Field–field velocity correlation

We would like to compute the correlation $\langle\phi_k\dot{\phi}_{k'}\rangle$. To accomplish this we first inspect the product:

$$\begin{aligned}\phi_k(z_1)\dot{\phi}_{k'}(z_2) = \phi_k(z_1)\Bigg(&-H^{-1}z_2^{\frac{1}{2}}\int_{z_i}^{z_2} ds\; s^{-\frac{3}{2}}\exp\left[\frac{A_{k'}}{2}(z_2-s_2)\right] \\ &\times\cos(z_2-s_2)\xi_{k'}(s_2) + \frac{H}{2}(1-A_{k'}z_2)\phi_{k'}(z_2)\Bigg).\end{aligned} \tag{D.18}$$

Where we used the expression for the field's velocity modes (D.3). As $\phi_k(z_2)$ contains a $\sin(s_2-z_2)$, when we take the average of the trigonometric function in the above equation only the second term will survive (cf. Section 6.2.1 and equation (D.8)).

So setting $z_1 = z_2 = z$ we are left with:

$$\begin{aligned}\langle\phi_k\dot{\phi}_{k'}\rangle &\approx \frac{H}{2}\Big(1-A_kz\Big)\,\langle\phi_k(z)\phi_{k'}(z)\rangle \\ &\approx -\frac{\Gamma_\phi}{2}\,\langle\phi_k(z)\phi_{k'}(z)\rangle\,.\end{aligned} \tag{D.19}$$

The last line follows because the second term in parenthesis is much larger than the first one.

The correlation between the field and field velocity is given in terms of their modes as:

$$\begin{aligned}\langle\phi(\boldsymbol{x})\dot{\phi}(\boldsymbol{y})\rangle &= \int \frac{d^3k}{(2\pi)^3}\frac{d^3k}{(2\pi)^3}\ \langle\phi_k\dot{\phi}_{k'}\rangle \exp(i\boldsymbol{k}\cdot\boldsymbol{x})\exp(i\boldsymbol{k}'\cdot\boldsymbol{y}) \\ \langle\phi(\boldsymbol{x})\dot{\phi}(\boldsymbol{y})\rangle &= -\frac{\Gamma_\phi T}{2a^3}\int \frac{d^3k}{(2\pi)^3}\ \frac{1}{\omega_k^2}\exp[i\boldsymbol{k}\cdot(\boldsymbol{x}-\boldsymbol{y})].\end{aligned} \tag{D.20}$$

Where used the correlation (D.19).

Elsewhere we will make use of the quantity:

$$\begin{aligned}\langle\phi(0)\dot{\phi}(\boldsymbol{x})\rangle^2 &= \frac{\Gamma_\phi^2 T^2}{4a^6}\int \frac{d^3k}{(2\pi)^3}\frac{d^3k'}{(2\pi)^3}\ \frac{1}{\omega_k^2}\frac{1}{\omega_{k'}^2}\exp[-i\boldsymbol{x}\cdot(\boldsymbol{k}+\boldsymbol{k}')], \\ &= \frac{\Gamma_\phi^2}{4}\langle\phi(0)\phi(\boldsymbol{x})\rangle^2\end{aligned} \tag{D.21}$$

so we leave it here for further reference.

D.4 Field–field gradient correlation

We write the correlation between the field and the field gradient in terms of their modes:

$$\begin{aligned}\langle\phi(\boldsymbol{x})\partial_i\phi(\boldsymbol{y})\rangle &= i\int \frac{d^3k}{(2\pi)^3}\frac{d^3k}{(2\pi)^3}\ k_i'\langle\phi_k\phi_{k'}\rangle \exp(i\boldsymbol{k}\cdot\boldsymbol{x})\exp(i\boldsymbol{k}'\cdot\boldsymbol{y}) \\ \langle\phi(\boldsymbol{x})\partial_i\phi(\boldsymbol{y})\rangle &= -i\frac{T}{a^3}\int \frac{d^3k}{(2\pi)^3}\ \frac{k_i}{\omega_k^2}\exp[i\boldsymbol{k}\cdot(\boldsymbol{x}-\boldsymbol{y})].\end{aligned} \tag{D.22}$$

Where once again, we used the variance of the field modes (6.23).

Elsewhere we will make use of the quantity:

$$\langle\phi(0)\partial_i\phi(\boldsymbol{x})\rangle^2 = -\frac{T^2}{a^6}\int \frac{d^3k}{(2\pi)^3}\frac{d^3k'}{(2\pi)^3}\ \frac{\boldsymbol{k}\cdot\boldsymbol{k}'}{\omega_k^2\omega_{k'}^2}\exp[-i\boldsymbol{x}\cdot(\boldsymbol{k}+\boldsymbol{k}')], \tag{D.23}$$

so we record it here for further reference.

D.5 Field velocity–field gradient correlation

We write the correlation between the field velocity and the field gradient in terms of their modes:

$$\begin{aligned}\langle\dot{\phi}(\boldsymbol{x})\partial_i\phi(\boldsymbol{y})\rangle &= i\int\frac{d^3k}{(2\pi)^3}\frac{d^3k}{(2\pi)^3}\,k_i'\,\langle\dot{\phi}_k\phi_{k'}\rangle\exp(i\boldsymbol{k}\cdot\boldsymbol{x})\exp(i\boldsymbol{k}'\cdot\boldsymbol{y})\\ \langle\dot{\phi}(\boldsymbol{x})\partial_i\phi(\boldsymbol{y})\rangle &= i\frac{\Gamma_\phi T}{2a^3}\int\frac{d^3k}{(2\pi)^3}\,\frac{k_i}{\omega_k^2}\exp[i\boldsymbol{k}\cdot(\boldsymbol{x}-\boldsymbol{y})].\end{aligned} \tag{D.24}$$

Where we applied the correlation computed above (D.19).

Elsewhere we will make use of the correlation:

$$\begin{aligned}\langle\dot{\phi}(0)\partial_i\phi(\boldsymbol{x})\rangle^2 &= -\frac{\Gamma_\phi^2T^2}{4a^6}\int\frac{d^3k}{(2\pi)^3}\frac{d^3k'}{(2\pi)^3}\,\frac{\boldsymbol{k}\cdot\boldsymbol{k}'}{\omega_k^2\omega_{k'}^2}\exp[-i\boldsymbol{x}\cdot(\boldsymbol{k}+\boldsymbol{k}')],\\ &= \frac{\Gamma_\phi^2}{4}\langle\phi(0)\partial_i\phi(\boldsymbol{x})\rangle^2,\end{aligned} \tag{D.25}$$

so we write it here for further reference.

Appendix E

Additional contributions to the power spectrum

Here we compute the remaining contributions to the curvature power spectrum $\mathcal{P}_\zeta$ appearing in equation (6.41). These contribution are related with the Fourier transform of the correlations computed in Section D. All of them will be affected by the transform in the same way, as presented in section 6.2.2 for the case of the field–field contribution. We present it here more generically for convenience.

The correlations have the typical form:

$$\langle X_i(0)X_j(\boldsymbol{x})\rangle^2 = \int \frac{d^3k_1}{(2\pi)^3}\frac{d^3k_2}{(2\pi)^3}\, f(\boldsymbol{k}_1,\boldsymbol{k}_2)\exp[-i\boldsymbol{x}\cdot(\boldsymbol{k}+\boldsymbol{k}')], \tag{E.1}$$

where we are omitting any prefactors in this sketch. We consider $X_1 = \phi$, $X_2 = \dot{\phi}$, $X_3 = \partial_i\phi$ and f is a function of $\boldsymbol{k}_1$ and $\boldsymbol{k}_2$. When we apply the Fourier transform it will make a delta function appear:

$$\int d^3x\ \exp(-i\boldsymbol{k}\cdot\boldsymbol{x})\,\langle X_i(0)X_j(\boldsymbol{x})\rangle^2 = \int \frac{d^3k_1}{(2\pi)^3}d^3k_2\ f(\boldsymbol{k}_1,\boldsymbol{k}_2)\delta(\boldsymbol{k}+\boldsymbol{k}_1+\boldsymbol{k}_2). \tag{E.2}$$

As the Fourier expansion of the delta Dirac function is given by:

$$\int d^3x\ \exp[i\boldsymbol{x}\cdot(-\boldsymbol{k}-\boldsymbol{k}_1-\boldsymbol{k}_2)] = (2\pi)^3\delta(\boldsymbol{k}+\boldsymbol{k}_1+\boldsymbol{k}_2), \tag{E.3}$$

this results in setting $\boldsymbol{k}_2 = -\boldsymbol{k}-\boldsymbol{k}_1$ and the contribution to $\mathcal{P}_\zeta$ reads:

$$\int d^3x\ \exp(-i\boldsymbol{k}\cdot\boldsymbol{x})\,\langle X_i(0)X_j(\boldsymbol{x})\rangle^2 = \int \frac{d^3k_1}{(2\pi)^3}d^3k_2\ f(\boldsymbol{k}_1,-\boldsymbol{k}-\boldsymbol{k}_1). \tag{E.4}$$

We now proceed to list all the contributions excluding the field-field contribution which has been already computed in the main text:

- **Kinetic–kinetic term:** Using the result (D.14) we obtain:

$$\begin{aligned}\int d^3x\ \exp(-i\boldsymbol{k}\cdot\boldsymbol{x})\frac{1}{2}\left\langle\dot{\phi}(0)\dot{\phi}(\boldsymbol{x})\right\rangle^2 &= \frac{1}{(2\pi)^2}\frac{T^2}{a^6}\int\frac{dk_1}{(2\pi)^3},\\ &= \frac{1}{(2\pi)^2}\frac{T^2}{a^6}\int_0^{\pi T_i} dk_1\ k_1^2,\\ &= \frac{\pi}{12}\frac{T^5}{a^3}.\end{aligned} \tag{E.5}$$

- **Gradient–gradient term:** Considering the quantity (D.17) we get:

$$\begin{aligned}\int d^3x\ \exp(-i\boldsymbol{k}\cdot\boldsymbol{x})\frac{1}{2}a^{-4}\left\langle\partial_i\phi(0)\partial_i\phi(\boldsymbol{x})\right\rangle^2 &= \frac{1}{2}\frac{T^2}{a^{10}}\int\frac{d^3k_1}{(2\pi)^3}\ \frac{[\boldsymbol{k}_1\cdot(\boldsymbol{k}+\boldsymbol{k}_1)]^2}{\omega_{k_1}^2\omega_{k+k_1}^2},\\ &= \frac{1}{2}\frac{T^2}{a^6}\int\frac{d^3k_1}{(2\pi)^3}\ \frac{\left(k_1^2+\boldsymbol{k}_1\cdot\boldsymbol{k}\right)^2}{k_1^2+\alpha^2T_i^2}\\ &\quad\times\frac{1}{(\boldsymbol{k}+\boldsymbol{k}_1)^2+\alpha^2T_i^2}.\end{aligned} \tag{E.6}$$

  This integral will be dominated by its upper limit so we can safely neglect $\boldsymbol{k}$ as we are interested in super-horizon modes:

$$\begin{aligned}\int d^3x\ \exp(-i\boldsymbol{k}\cdot\boldsymbol{x})\frac{1}{2}a^{-4}\left\langle\partial_i\phi(0)\partial_i\phi(\boldsymbol{x})\right\rangle^2 &\approx \frac{1}{(2\pi)^2}\frac{T^2}{a^6}\int_0^{\pi T_i} dk_1\\ &\quad\times\frac{k_1^6}{\left(k_1^2+\alpha^2T_i^2\right)^2},\\ &\approx\frac{\alpha^3}{(2\pi)^2}\frac{T^5}{a^3}\left[-2\frac{\pi}{\alpha}+\frac{\pi^3}{3\alpha^3}-\frac{\alpha\pi}{2(\alpha^2+\pi^2)}+\frac{5}{2}\arctan\left(\pi\alpha^{-1}\right)\right].\end{aligned} \tag{E.7}$$

- **Field–kinetic term:** Invoking the correlation (D.21) we find that we can write this contribution in terms of the field–field one:

$$\begin{aligned}\int d^3x\ \exp(-i\boldsymbol{k}\cdot\boldsymbol{x})\alpha^2T^2\left\langle\phi(0)\dot{\phi}(\boldsymbol{x})\right\rangle^2 &= \frac{\Gamma_\phi^2}{2T^2\alpha^2}\int d^3x\ \exp(-i\boldsymbol{k}\cdot\boldsymbol{x})\\ &\quad\times\frac{1}{2}\alpha^4T^4\left\langle\phi(0)\phi(\boldsymbol{x})\right\rangle^2,\\ &= \frac{1}{2}\left(\frac{3\alpha^3}{16\pi}\right)^2\int d^3x\ \exp(-i\boldsymbol{k}\cdot\boldsymbol{x})\\ &\quad\times\frac{1}{2}\alpha^4T^4\left\langle\phi(0)\phi(\boldsymbol{x})\right\rangle^2.\end{aligned} \tag{E.8}$$

- **Field–gradient term:** Recalling (D.23) we obtain:

$$\begin{aligned}\int d^3x\ \exp(-i\boldsymbol{k}\cdot\boldsymbol{x})a^{-2}\alpha^2T^2\left\langle\phi(0)\partial_i\phi(\boldsymbol{x})\right\rangle^2 &= \frac{\alpha^2T^4}{a^8}\int\frac{d^3k_1}{(2\pi)^3}\frac{\boldsymbol{k}_1\cdot(\boldsymbol{k}_1+\boldsymbol{k})}{\omega_k^2\omega_{k+k_1}^2},\\ &= \frac{\alpha^2T^4}{a^4}\int\frac{d^3k_1}{(2\pi)^3}\frac{k_1^2+\boldsymbol{k}_1\cdot\boldsymbol{k}}{k_1^2+\alpha^2T_i^2},\\ &\quad\times\frac{1}{(\boldsymbol{k}+\boldsymbol{k}_1)^2+\alpha^2T_i^2}.\end{aligned} \tag{E.9}$$

We are considering super-horizon modes so it is safe to neglect $\boldsymbol{k}$:

$$\begin{aligned}\int d^3x\ \exp(-i\boldsymbol{k}\cdot\boldsymbol{x})a^{-2}\alpha^2T^2\left\langle\phi(0)\partial_i\phi(\boldsymbol{x})\right\rangle^2 &\approx \frac{2}{(2\pi)^2}\frac{\alpha^2T^4}{a^4}\int_0^{\pi T_i}dk_1\\ &\quad\times\frac{k_1^4}{\left(k_1^2+\alpha^2T_i^2\right)^2},\\ &\approx\frac{2\alpha^3}{(2\pi)^2}\frac{T^5}{a^3}\left[\frac{\pi}{\alpha}+\frac{\alpha\pi}{2\left(\alpha^2+\pi^2\right)}-\frac{3}{2}\arctan\left(\pi\alpha^{-1}\right)\right].\end{aligned} \tag{E.10}$$

- **Kinetic–gradient term :** Recalling (D.25) we see that this contribution can be written in terms of the field–gradient one:

$$\begin{aligned}\int d^3x\ \exp(-i\boldsymbol{k}\cdot\boldsymbol{x})a^{-2}\left\langle\dot\phi(0)\partial_i\phi(\boldsymbol{x})\right\rangle^2 &= \frac{\Gamma_\phi^2}{4\alpha^2T^2}\int d^3x\ \exp(-i\boldsymbol{k}\cdot\boldsymbol{x})\\ &\quad\times a^{-2}\alpha^2T^2\left\langle\phi(0)\partial_i\phi(\boldsymbol{x})\right\rangle^2,\\ &= \left(\frac{3\alpha^3}{32\pi}\right)^2\int d^3x\ \exp(-i\boldsymbol{k}\cdot\boldsymbol{x})\\ &\quad\times a^{-2}\alpha^2T^2\left\langle\phi(0)\partial_i\phi(\boldsymbol{x})\right\rangle^2.\end{aligned} \tag{E.11}$$

Bibliography

[1] Scott Dodelson and Fabian Schmidt. *Modern Cosmology*. Pittsburgh: Academic Press, 2019. ISBN: 978-0-12-815948-4.

[2] Edward W. Kolb and Michael S. Turner. *The Early Universe*. Vol. 69. 1990. ISBN: 978-0-201-62674-2.

[3] Daniel Baumann. "Inflation". In: *Theoretical Advanced Study Institute in Elementary Particle Physics: Physics of the Large and the Small*. 2011, pp. 523–686. DOI: 10.1142/9789814327183_0010. arXiv: 0907.5424 [hep-th].

[4] João G. Rosa. "Introduction to Cosmology". Lecture 1-13. URL: http://gravitation.web.ua.pt/node/247.

[5] David H. Lyth and Ewan D. Stewart. "Cosmology with a TeV mass GUT Higgs". In: *Phys. Rev. Lett.* 75 (1995), pp. 201–204. DOI: 10.1103/PhysRevLett.75.201. arXiv: hep-ph/9502417.

[6] David H. Lyth and Ewan D. Stewart. "Thermal inflation and the moduli problem". In: *Phys. Rev. D* 53 (1996), pp. 1784–1798. DOI: 10.1103/PhysRevD.53.1784. arXiv: hep-ph/9510204.

[7] B. J. Carr and S. W. Hawking. "Black Holes in the Early Universe". In: *Monthly Notices of the Royal Astronomical Society* 168.2 (Aug. 1974), pp. 399–415. ISSN: 0035-8711. DOI: 10.1093/mnras/168.2.399. eprint: https://academic.oup.com/mnras/article-pdf/168/2/399/8079885/mnras168-0399.pdf. URL: https://doi.org/10.1093/mnras/168.2.399.

[8] Sebastien Clesse and Juan García-Bellido. "Seven Hints for Primordial Black Hole Dark Matter". In: *Phys. Dark Univ.* 22 (2018), pp. 137–146. DOI: 10.1016/j.dark.2018.08.004. arXiv: 1711.10458 [astro-ph.CO].

[9] Bernard Carr and Florian Kuhnel. "Primordial Black Holes as Dark Matter: Recent Developments". In: (June 2020). DOI: 10.1146/annurev-nucl-050520-125911. arXiv: 2006.02838 [astro-ph.CO].

[10] Konstantinos Dimopoulos et al. "Primordial Black Holes from Thermal Inflation". In: *JCAP* 07 (2019), p. 046. DOI: 10.1088/1475-7516/2019/07/046. arXiv: 1903.09598 [astro-ph.CO].

[11] Michel Le Bellac. *Thermal Field Theory*. Cambridge Monographs on Mathematical Physics. Cambridge University Press, Mar. 2011. ISBN: 978-0-511-88506-8, 978-0-521-65477-7. DOI: 10.1017/CBO9780511721700.

[12] J.I. Kapusta and Charles Gale. *Finite-temperature field theory: Principles and applications*. Cambridge Monographs on Mathematical Physics. Cambridge University Press, 2011. ISBN: 978-0-521-17322-3, 978-0-521-82082-0, 978-0-511-22280-1. DOI: 10.1017/CBO9780511535130.

[13] Arjun Berera, Ian G. Moss, and Rudnei O. Ramos. "Warm Inflation and its Microphysical Basis". In: *Rept. Prog. Phys.* 72 (2009), p. 026901. DOI: 10.1088/0034-4885/72/2/026901. arXiv: 0808.1855 [hep-ph].

[14] João G. Rosa. "Non-equilibrium Quantum Field Theory and cosmological applications". URL: http://gravitation.web.ua.pt/sites/default/files/migrated2016/Non-equilibrium_QFT.pdf.

[15] V. Mukhanov. *Physical Foundations of Cosmology*. Oxford: Cambridge University Press, 2005. ISBN: 978-0-521-56398-7.

[16] Steven Weinberg. *Cosmology*. Sept. 2008. ISBN: 978-0-19-852682-7.

[17] M. Roos. *Introduction to cosmology*. 3rd edition. 2003.

[18] Edwin Hubble. "A relation between distance and radial velocity among extragalactic nebulae". In: *Proceedings of the National Academy of Sciences* 15.3 (1929), pp. 168–173. ISSN: 0027-8424. DOI: 10.1073/pnas.15.3.168. eprint: https://www.pnas.org/content/15/3/168.full.pdf. URL: https://www.pnas.org/content/15/3/168.

[19] Arno A. Penzias and Robert Woodrow Wilson. "A Measurement of excess antenna temperature at 4080-Mc/s". In: *Astrophys. J.* 142 (1965), pp. 419–421. DOI: 10.1086/148307.

[20] M. Tanabashi et al. "Review of Particle Physics". In: *Phys. Rev. D* 98 (3 Aug. 2018), p. 030001. DOI: 10.1103/PhysRevD.98.030001. URL: https://link.aps.org/doi/10.1103/PhysRevD.98.030001.

[21] D.J. Fixsen. "The Temperature of the Cosmic Microwave Background". In: *Astrophys. J.* 707 (2009), pp. 916–920. DOI: 10.1088/0004-637X/707/2/916. arXiv: 0911.1955 [astro-ph.CO].

[22] Sean M. Carroll. *Spacetime and Geometry*. Cambridge University Press, July 2019. ISBN: 978-0-8053-8732-2, 978-1-108-48839-6, 978-1-108-77555-7.

[23] Robert M. Wald. *General Relativity*. Chicago, USA: Chicago Univ. Pr., 1984. DOI: 10.7208/chicago/9780226870373.001.0001.

[24] N. Aghanim et al. "Planck 2018 results. VI. Cosmological parameters". In: (July 2018). arXiv: 1807.06209 [astro-ph.CO].

[25] Sohrab Rahvar. "Cooling in the universe". In: (Mar. 2006). arXiv: physics/0603087.

[26] Andrei D. Linde. *Particle physics and inflationary cosmology*. Vol. 5. 1990. arXiv: hep-th/0503203.

[27] Lars Bergström. "Nonbaryonic dark matter: Observational evidence and detection methods". In: *Rept. Prog. Phys.* 63 (2000), p. 793. DOI: 10.1088/0034-4885/63/5/2r3. arXiv: hep-ph/0002126.

[28] Joshua Frieman, Michael Turner, and Dragan Huterer. "Dark Energy and the Accelerating Universe". In: *Ann. Rev. Astron. Astrophys.* 46 (2008), pp. 385–432. DOI: 10.1146/annurev.astro.46.060407.145243. arXiv: 0803.0982 [astro-ph].

[29] Ruediger Vaas. "Dark energy and life's ultimate future". In: Mar. 2007, pp. 4967–5. arXiv: physics/0703183.

[30] Alan H. Guth. "The Inflationary Universe: A Possible Solution to the Horizon and Flatness Problems". In: *Adv. Ser. Astrophys. Cosmol.* 3 (1987). Ed. by Li-Zhi Fang and R. Ruffini, pp. 139–148. DOI: 10.1103/PhysRevD.23.347.

[31] Andrei D. Linde. "A New Inflationary Universe Scenario: A Possible Solution of the Horizon, Flatness, Homogeneity, Isotropy and Primordial Monopole Problems". In: *Adv. Ser. Astrophys. Cosmol.* 3 (1987). Ed. by Li-Zhi Fang and R. Ruffini, pp. 149–153. DOI: 10.1016/0370-2693(82)91219-9.

[32] Daniel Baumann and Hiranya V. Peiris. "Cosmological Inflation: Theory and Observations". In: *Adv. Sci. Lett.* 2 (2009), pp. 105–120. DOI: 10.1166/asl.2009.1019. arXiv: 0810.3022 [astro-ph].

[33] Andrei D. Linde. "Inflation and string cosmology". In: *Prog. Theor. Phys. Suppl.* 163 (2006). Ed. by Miguel Alcubierre, Jorge L. Cervantes-Cota, and Merced Montesinos, pp. 295–322. DOI: 10.1143/PTPS.163.295. arXiv: hep-th/0503195.

[34] Takashi Hiramatsu, Yuhei Miyamoto, and Jun'ichi Yokoyama. "Effects of thermal fluctuations on thermal inflation". In: *JCAP* 03 (2015), p. 024. DOI: 10.1088/1475-7516/2015/03/024. arXiv: 1412.7814 [hep-ph].

[35] Tiago Barreiro et al. "Some aspects of thermal inflation: The Finite temperature potential and topological defects". In: *Phys. Rev. D* 54 (1996), pp. 1379–1392. DOI: 10.1103/PhysRevD.54.1379. arXiv: hep-ph/9602263.

[36] D. Bailin and A. Love. *Supersymmetric gauge field theory and string theory*. Oct. 1994.

[37] D.H. Lyth. "A Bound on Inflationary Energy Density From the Isotropy of the Microwave Background". In: *Phys. Lett. B* 147 (1984). [Erratum: Phys.Lett.B 150, 465 (1985)], p. 403. DOI: 10.1016/0370-2693(84)91391-1.

[38] Andrew R. Liddle. "The Inflationary energy scale". In: *Phys. Rev. D* 49 (1994), pp. 739–747. DOI: 10.1103/PhysRevD.49.739. arXiv: astro-ph/9307020.

[39] Lisa Randall and Scott D. Thomas. "Solving the cosmological moduli problem with weak scale inflation". In: *Nucl. Phys. B* 449 (1995), pp. 229–247. DOI: 10.1016/0550-3213(95)00228-K. arXiv: hep-ph/9407248.

[40] Michael Dine, Lisa Randall, and Scott D. Thomas. "Baryogenesis from flat directions of the supersymmetric standard model". In: *Nucl. Phys. B* 458 (1996), pp. 291–326. DOI: 10.1016/0550-3213(95)00538-2. arXiv: hep-ph/9507453.

[41] L. Dolan and R. Jackiw. "Symmetry Behavior at Finite Temperature". In: *Phys. Rev. D* 9 (1974), pp. 3320–3341. DOI: 10.1103/PhysRevD.9.3320.

[42] Mar Bastero-Gil et al. "The role of fluctuation-dissipation dynamics in setting initial conditions for inflation". In: *JCAP* 01 (2018), p. 002. DOI: 10.1088/1475-7516/2018/01/002. arXiv: 1612.04726 [astro-ph.CO].

[43] Mar Bastero-Gil, Arjun Berera, and Rudnei O. Ramos. "Dissipation coefficients from scalar and fermion quantum field interactions". In: *JCAP* 09 (2011), p. 033. DOI: 10.1088/1475-7516/2011/09/033. arXiv: 1008.1929 [hep-ph].

[44] J. William Byrd. "Introducing Green's function for initial- and boundary-value problems". In: *American Journal of Physics* 44.6 (June 1976), pp. 596–597. DOI: 10.1119/1.10367.

[45] Dean G. Duffy. *Green's Functions With Applications*. 2nd edition. 2015.

[46] George B. Arfken, Hans J. Weber, and Frank E. Harris. *Mathematical Methods for Physicists*. Pittsburgh: Academic Press, 2012. ISBN: 978-0-12-384654-9.

[47] George F. Simmons. *Differential Equations with Applications and Historical Notes*. 3rd edition. 2017.

[48] Milton Abramowitz and Irene A. Stegun. *Handbook of Mathematical Functions. Formulas, Graphs and Mathematical Tables*. 10th edition. 1972.

[49] Daniel Zwillinger. *Handbook of Differential Equations*. 3rd edition. 1997.

[50] Rick Durrett. *Probability*. 2019. ISBN: 978-1-108-47368-2.

[51] L. Isserlis. *On a Formula for the Product-Moment Coefficient of any Order of a Normal Frequency Distribution in any Number of Variables*. Nov. 1918. DOI: 10.2307/2331932. URL: https://zenodo.org/record/1431593.

[52] C. Vignat. "A generalized Isserlis theorem for location mixtures of Gaussian random vectors". In: *Statistics & Probability Letters* 82.1 (Jan. 2012), pp. 67–71. ISSN: 0167-7152. DOI: 10.1016/j.spl.2011.09.008. arXiv: 1107.2309 [math.PR].

[53] Andrei D. Linde. "Fast roll inflation". In: *JHEP* 11 (2001), p. 052. DOI: 10.1088/1126-6708/2001/11/052. arXiv: hep-th/0110195.